

PARTICLE, KINETIC AND FLUID MODELS FOR PHOTOTAXIS

SEUNG-YEAL HA

Department of Mathematical Sciences
Seoul National University
Seoul 151-747, Korea

DORON LEVY

Department of Mathematics
and Center for Scientific Computation and Mathematical Modeling
University of Maryland
College Park, MD 20742, USA

(Communicated by Benoit Perthame)

ABSTRACT. In this work we derive a hierarchy of new mathematical models for describing the motion of phototactic bacteria, i.e., bacteria that move towards light. These models are based on recent experiments suggesting that the motion of such bacteria depends on the individual bacteria, on group dynamics, and on the interaction between bacteria and their environment. Our first model is a collisionless interacting *particle system* in which we follow the location of the bacteria, their velocity, and their internal excitation (a parameter whose role is assumed to be related to communication between bacteria). In this model, the light source acts as an external force. The resulting particle system is an extension of the Cucker-Smale flocking model. We prove that when all particles are fully excited, their asymptotic velocity tends to an identical (pre-determined) terminal velocity. Our second model is a *kinetic model* for the one-particle distribution function that includes an internal variable representing the excitation level. The kinetic model is a Vlasov-type equation that is derived from the particle system using the BBGKY hierarchy and molecular chaos assumption. Since bacteria tend to move in areas that were previously traveled by other bacteria, a surface memory effect is added to the kinetic model as a turning operator that accounts for the collisions between bacteria and the environment. The third and final model is derived as a formal macroscopic limit of the kinetic model. It is shown to be the *Vlasov-McKean equation* coupled with a reaction-diffusion equation.

1. Introduction. Microorganisms live in environments that are often severely limited in resources or in which vital inputs such as light and nutrients fluctuate unpredictably. An example of such an organism is cyanobacteria, a photosynthetic microorganism that has the ability to sense and respond to changes in the intensity of light and its direction, a processes that is called “phototaxis”. Under certain conditions these bacteria will initiate a motion towards a light source. This work is

2000 *Mathematics Subject Classification.* Primary: 92C17; Secondary: 82C22, 82C40.

Key words and phrases. Phototaxis, Chemotaxis, Particle systems, Kinetic models, Vlasov equation, Vlasov-McKean equation, Cucker-Smale model, Flocking.

The work of S.-Y. Ha was supported in part by KOSEF R01-2006-000-10002-0. The work of D. Levy was supported in part by the NSF under Career Grant DMS-0133511, and by the joint NSF/NIGMS program under Grant Number DMS-0758374.

motivated by the recent experiments of Burriesci and Bhaya [10] in which time-lapse video microscopy was used to monitor the movement of a particular phototactic cyanobacterium, *Synochocystis* sp. Strain PCC6803. These experiments indicate that the motion of the colony of bacteria is not a simple function of the response to the light of an individual bacterium. In fact, the resulting dynamics turns out to be a complex function of the state of the system, the motion characteristics of individual bacteria, group dynamics between neighboring bacteria, and interactions between bacteria and the environment. The extensive experimental work that has been conducted over the past decade has substantially increased the knowledge-base on phototactic bacteria in various directions (such as the existence of type IV pili, cAMP, photoreceptors, ...) (see, e.g., [1, 5, 6, 8, 9, 11, 27, 29, 30, 31, 32, 38, 39, 40, 41, 42] and the references therein). Yet, very little is known about how these components can be integrated in order to explain some of the observed phenomena during phototaxis.

Our main goal in this work is to develop mathematical models for describing phototaxis. The mathematical work attempts to provide an analytical framework for studying hypotheses on the mechanisms that control phototaxis, as well as a framework for conducting theoretical studies that exceed the present capabilities of the wet lab. The field of mathematical models for cell motility, has been rapidly growing over the past several decades. Most notable are the mathematical models for chemotaxis (a situation where the organism moves in the direction of the gradient of the chemical concentration of their nutrients). In that field, the fundamental model is the celebrated Keller-Segel model for chemotaxis [21, 22] (also derived by Patlak [33]). It is beyond the scope of this introduction to provide a comprehensive overview of the recent advancements on the mathematical theory of chemotaxis. Instead we refer the interested reader to the review article [20] and to the references therein. Mathematical models of phototaxis are still rather sparse. A couple of isolated examples include [14] and [28], none of which considers the group dynamics as a mechanism that is related to the motion. Recently, in a series of papers, Levy and Requeijo introduced stochastic models for describing phototaxis, [7, 24, 25]. The approach that was taken in these works was to consider the bacteria as a system of stochastically interacting particles. The work [24] was devoted to deriving a system of PDEs for describing phototaxis as the limit of a stochastically interacting many particle system. The resulting system of PDEs resembled the Keller-Segel model for chemotaxis [22]. Extensive numerical simulations of the discrete models were conducted in [25].

In this work we develop a hierarchy of models for phototaxis based on the experiments of Burriesci and Bhaya. These models incorporate a flocking mechanism. “Flocking” represents the phenomenon in which self-propelled individuals using only limited environmental information and simple rules, organize into an ordered motion (see [15, 16]). The first model we derive is a collisionless interacting particle system. This model is formulated as a system of ODEs that describe the time evolution of the locations of the bacteria, their velocities, and the excitation of each bacterium. The forces that control the dynamics of the velocities and of the excitation are divided into external and internal forces. For this model we prove that asymptotically, one can expect a flocking behavior for the particles, i.e., a motion for which all particles move towards the light source with identical velocities. This result is true, at least for the case when all particles are fully excited. The particle model can be seen as an extension of the Cucker-Smale flocking model [15, 16, 17, 37], which

is precisely what it boils down to in the absence of external forcing (i.e., without light).

The second model is a kinetic, Vlasov-type, model based on the interacting particle system model. First, we derive a collisionless kinetic model using the BBGKY hierarchy with the standard closure due to a molecular chaos assumption. Similar to the particle system, we also prove the flocking property of the kinetic model under the assumption that all particles are fully excited. We then add collisions due to the interaction of particles with the environment. These “collisions” incorporate into the model a surface memory effect (that is experimentally observed). It enters into the model in the form of a turning operator. This work is related to the recent kinetic formulation of the Cucker-Smale model due to Ha and Tadmor [18].

The third model is a macroscopic (fluid) model that is formally derived from the kinetic model. Due to the non-local terms that represent the interaction of the particles with their neighbors, the resulting model turns out to be the Vlasov-McKean equation for the density of the particles, coupled with a reaction diffusion equation for the surface memory effect. Certain parts of the derivation are based on the work of Hillen, *et al.* [19] on chemotaxis. We note in passing that kinetic models have been playing an increasingly important role in mathematical models of biological systems, and in particular in modeling of cell movement. See, e.g., the books [2, 3, 34] and the references therein.

The structure of the paper is as follows: In Section 2 we summarize the experimental observations of Burriesci and Bhaya [10]. These experimental observations lead us to formulate hypotheses on which the mathematical derivation is based. In Section 3 we introduce the collisionless interacting particle system. This system describes the dynamics of the location of particles, their velocity, and their excitation. In this section we also present results of numerical simulations that were conducted in order to demonstrate the emerging dynamics of our interacting particle system. The kinetic model is then derived in Section 4, first for a collisionless system, to which we then add collisions with the environment. In Section 5 we derive a fluid model as the formal limit of the kinetic model. The fluid model turns out to be a Vlasov-McKean type equation (coupled with a reaction-diffusion equation for the surface memory effect). Concluding comments are provided in Section 6.

2. Background: Observations and assumptions. In [10] Bhaya and Burriesci used time-lapse video microscopy to track the movement of cells. An analysis of these videos has led us to various observations regarding the characteristics of the motion. Here we provide a brief summary of the main observations. More details can be found in [24, 25].

1. *Delayed motion.* Even when light is on, it still takes a long time (minutes to hours) for a bacterium to initiate a motion towards the light source. When such motion develops, it is always observed in areas of a relatively high-density of bacteria. Individual bacterium will almost never initiate a motion towards light.
2. *Fingering.* When the bacterial colony starts moving towards the light source, in certain cases it tends to form *fingers* such as those that are shown in Figure 1. This happens mostly when the initial distribution is inhomogeneous and contains regions of high density and low density of bacteria. Bacteria that end up on the edges of these fingers seem to stop moving (or move very

slowly). In some cases it is even possible to observe *pinching* of the tip from the rest of the finger.

3. *Density-dependent motion.* When the density of the cells is high, bacteria tend to move in one group towards the light (see Figure 2). No clear preferred movement direction is observed if the density of bacteria is low.
4. *A surface memory effect.* The movies suggest that when cells move, they mark the surface in a way that makes it more likely for other cells to revisit locations that were already traveled by other bacteria. The precise mechanism for the marking of the surface with this particular strain of bacteria is unknown. A detailed discussion can be found in [25].
5. *Sensing other bacteria.* Some movies suggest that cells can sense other close-by cells even when they are not in physical contact. An example is shown in Figure 3. Cells that are located on the upper-left corner are stationary before the cells from the back get closer. They start moving before any direct physical contact is made with the other cells.

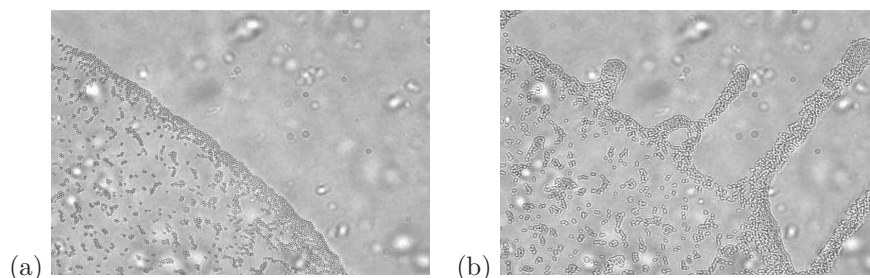


FIGURE 1. Fingering. The light source is at the upper-right corner of the domain. Figure (a) shows the edge of the colony with single cells showing as dark dots. Figure (b) shows the fingers that are created from the areas of initial higher density.

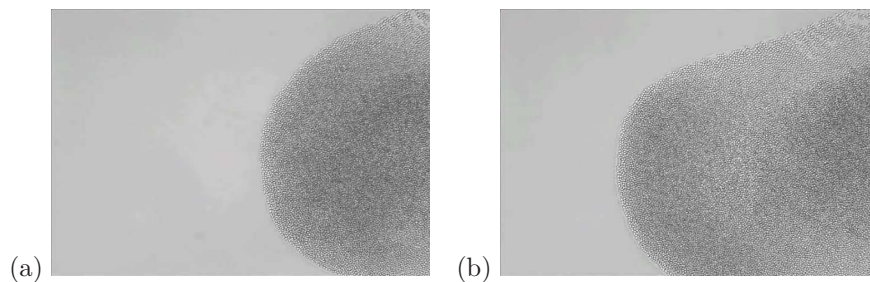


FIGURE 2. Bacteria motion when the density is high. The snapshots were taken at increasing times. The light source is to the left of the domain.

Based on the experimental observations, we formulate the following hypotheses regarding the mechanisms that determine the rules of motion during phototaxis.

1. **Communication and excitation.** We assume that there exists some form of communication between bacteria. The mechanism proposed to describe such

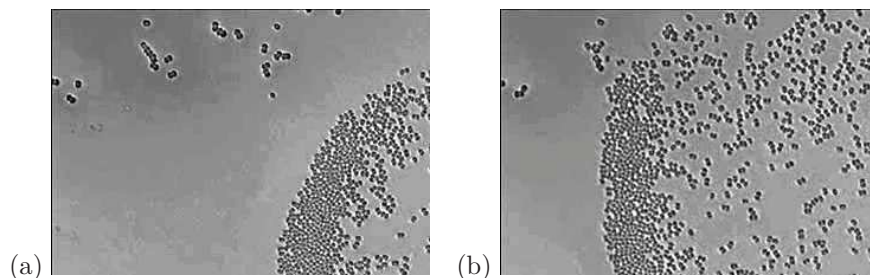


FIGURE 3. The cells on the upper-left corner stay stationary before the cells from the back approach them. They then start moving before making any physical contact with the moving cells. The light source is to the left of the domain.

communication is the existence of an *excitation* level that is associated with each cell. Excluding random phenomena, cells move only when the excitation exceeds over a critical threshold. The excitation associated with a given cell depends on the excitation of the surrounding bacteria. Delayed motion is then a consequence of the time it takes cells to build up the excitation that is required to initiate the motion.

2. **Surface memory.** We assume that cells mark the surface (possibly with some substance they produce) in a way that facilitates the motion of other cells. This surface marking should also influence cells in a way that they are more likely to revisit previously occupied locations. An expected consequence of such a surface memory effect is a system with fairly well-defined interfaces. In addition to a preferable motion towards previously occupied locations, cells are observed to move faster on such areas.

3. A collisionless interacting particle system. In this section, we present an external driven interacting particle system for modeling phototaxis. This particle system is based on some of the observations and the corresponding hypotheses that were described in Section 2.

The system derived here is a collisionless system in the sense that we describe the dynamics of particles that are assumed not to collide with each other and not to collide with the environment. As explained in Section 2, one of the factors that control the motion of the bacteria is their tendency to travel on areas that were previously visited by other bacteria. Since we view the surface as part of the environment, its influence on the dynamics is ignored in this section. The “surface memory effect” will be added to the model at a later stage when we allow for collisions between particles and the environment.

The main ingredients that will be included in the derivation of the particle system here are:

1. The light source. Bacteria are assumed to be stimulated due to the light source. In the particle system the light source will be treated as an external force.
2. The excitation of each bacterium. Bacteria are assumed to have an hidden internal property, which we refer to as “excitation”. This excitation should pass over a critical threshold for the bacteria to initiate a motion towards

the light source. The excitation of each bacterium will be adjusted over time based on the excitation of its immediate neighbors.

We would like to emphasize that the particular choice of the model is rather arbitrary. In this work, our main goal is to derive a model that incorporates the observations and assumptions rather than obtaining such a model from first principles.

3.1. Modeling a particle system. Let $(x_i, v_i) \in \mathbb{R}^{2d}$ be the phase-space position of particle number i . This particle has an associated scalar excitation level $\zeta_i \geq 0$. Consider a general form of a dynamical system $\{(x_i(t), v_i(t), \zeta_i(t))\}_{i=1}^N$:

$$\frac{dx_i}{dt} = v_i, \quad \frac{dv_i}{dt} = F^i, \quad \frac{d\zeta_i}{dt} = G^i, \quad i = 1, \dots, N. \quad (1)$$

Here, the mass of particles is assumed to be unity. F^i and G^i denote the force and excitation rate functions acting on i -particle, respectively. The issue at this point is to supply model constitutive relations for F^i and G^i that will dynamically reflect the observations and hypotheses.

Our first step is to model F^i . We decompose the force F^i into the sum of two forces: an inter-particle force F_{in}^i and an external body force F_{ex}^i . For the inter-particle force, we employ a flocking relaxation mechanism [15, 16, 18] which in the simpler setting described in these sources does generate an internal ‘‘flocking’’ mechanism for the particles:

$$F_{in}^i \equiv \frac{\lambda_1}{N} \sum_{j=1}^N k_1(x_j, x_i)(v_j - v_i), \quad \lambda_1 > 0. \quad (2)$$

Here, the kernel, k_1 , is a nonnegative, symmetric function satisfying

$$k_1 \in L_+^\infty(\mathbb{R}^{2d}), \quad k_1(x_j, x_i) = k_1(x_i, x_j), \quad 1 \leq i, j \leq N. \quad (3)$$

k_1 can be used, e.g., to describe the density dependent motion that was mentioned in Observation 3, as well as the observation regarding sensing other bacteria (Observation 5). As of the external force, it is assumed to be due to the light source, which is located at $|x| = \infty$. The light source points in the direction of a unit vector \hat{e}_s , and its intensity, I_0 , is assumed to be constant on the configuration domain under consideration. Due to the delay effect (1) in Section 2, we introduce a cut-off function so that the external force is effective after the excitation level of i -particle exceeds a priori determined threshold $\zeta_{cr} > 0$, i.e.,

$$F_{ex}^i \equiv I_0(u_\infty \hat{e}_s - v_i)(1 - \varphi(\zeta_i; \zeta_{cr})). \quad (4)$$

Here, $u_\infty = u_\infty(I_0)$ is a predetermined terminal speed and $\varphi(\cdot; \zeta_{cr})$ is any smooth cut-off function satisfying

$$\varphi(\zeta_i; \zeta_{cr}) = \begin{cases} 1, & \zeta_i \leq \zeta_{cr}, \\ 0, & \zeta_i > 2\zeta_{cr}. \end{cases} \quad 0 \leq \varphi \leq 1.$$

The dynamics of the particle system is assumed to be dominated by the external force that is due to the light source time-asymptotically. In this context, the self-oriented flocking mechanism should play a more minor effect. The coefficient 2 in the definition of φ is of no particular significance. Any number greater than 1 will work.

Remark 1.

In [15, 16, 18] bounded algebraically decaying functions were employed for the modeling of k_1 , i.e.,

$$k_1(x_j, x_i) = \frac{1}{(1 + |x_j - x_i|^2)^\beta}, \quad \beta \geq 0. \quad (5)$$

However, in our framework the explicit form of k_1 is irrelevant as long as it satisfies the property (3). In contrast, in the absence of external forces such as a light source, the internal flocking mechanism is rather sensitive to the choice of k_1 (see [15, 16, 18]).

We now proceed to model G^i in (1). Similarly to the previous case (F^i), the excitation level is also assumed to be affected by the excitation levels of neighboring particles (internal mechanism) and by an external source (external mechanism). In this case, for the internal mechanism, the excitation level of each particle is modified such that it is adjusted towards the averaged value of the excitation in its neighborhood. That is, when a particle interacts with particles with lower (higher) excitation levels, the excitation level of that particle will be decreased (increased). Based on these arguments, we assume the following internal excitation orientation mechanism of the form

$$G_{in}^i := \frac{\lambda_2}{N} \sum_{j=1}^N k_2(x_j, x_i)(\zeta_j - \zeta_i), \quad \lambda_2 \geq 0.$$

The kernel, k_2 , is a nonnegative symmetric function satisfying

$$k_2 \in L_+^\infty(\mathbb{R}^{2d}), \quad k_2(x_j, x_i) = k_2(x_i, x_j), \quad 1 \leq i, j \leq N.$$

In contrast, the light source is the external mechanism that is set to increase the excitation of the particles. Indeed, starting, e.g., with a set of particles, all with zero excitation, the light functions as the external force that gradually increases the excitation of all particles. To prevent an unlimited increase in the value of the excitation, we assume that it can increase (due to the light source) based on a certain capacity level, ζ_{cp} . We thus impose the following ansatz:

$$G_{ex}^i := I_0 \varphi(\zeta_i; \zeta_{cp}). \quad (6)$$

The role of this external force, G_{ex}^i should be thought of as an initialization mechanism for the excitation. Once the excitation of particles is no longer zero, the excitation of particles that are close to each other will increase more rapidly and a group motion will form. We now combine (1) - (6) to get the resulting dynamical system: For $i = 1, \dots, N$, $t \in \mathbb{R}_+$,

$$\begin{aligned} \frac{dx_i}{dt} &= v_i, \\ \frac{dv_i}{dt} &= \frac{\lambda_1}{N} \sum_{j=1}^N k_1(x_j, x_i)(v_j - v_i) + I_0(u_\infty \hat{e}_s - v_i)(1 - \varphi(\zeta_i; \zeta_{cr})), \\ \frac{d\zeta_i}{dt} &= \frac{\lambda_2}{N} \sum_{j=1}^N k_2(x_j, x_i)(\zeta_j - \zeta_i) + I_0 \varphi(\zeta_i; \zeta_{cp}). \end{aligned} \quad (7)$$

Here, I_0 is the constant intensity of the light source, u_∞ is the terminal speed of particles, ζ_{cr} is the critical excitation value, and ζ_{cp} is the excitation capacity.

Remark 2. In general, the light intensity is a function of the position. It is also known that the response of the bacteria may depend on the light intensity. For example, if the light intensity is greater than a certain threshold, the environment can be considered to be saturated with light, and the bacterial colony will not move at all. Such a dependence on the light intensity can be easily incorporated into the model. However, in order to simplify the presentation at this point, we assume that I_0 is a uniform on the domain under consideration.

Remark 3. In the absence of any light sources and without the excitation, the system (7) reduces to the Cucker-Smale's flocking system [15, 16, 18, 37]:

$$\begin{aligned}\frac{dx_i}{dt} &= v_i, \\ \frac{dv_i}{dt} &= \frac{\lambda_1}{N} \sum_{j=1}^N k_1(x_j, x_i)(v_j - v_i).\end{aligned}\tag{8}$$

We would like to emphasize that the system (7) is constructed in a way that the external forces are more dominant than the internal forces (which are the only forces that exist in the Cucker-Smale model (8)). To understand this, one can think of the situation in which the initial velocities for all particles are identically zero. If this is the case, in the Cucker-Smale model the velocities remain zero for all time. In our model, however, the velocities will still increase due to the external forcing. Once the velocities increase, other mechanisms kick in, and so on.

3.2. Time-asymptotic external flocking. In this section, we present several a priori estimates and study the emergent time-asymptotic flocking of the dynamical system (7).

Lemma 3.1. *Let (x_i, v_i, ζ_i) be the solution to the system (7). Then we have*

$$\begin{aligned}(i) \quad & \frac{d}{dt} \sum_{i=1}^N v_i = I_0 \left[\sum_{i=1}^N (u_\infty \hat{e}_s - v_i)(1 - \varphi(\zeta_i; \zeta_{cr})) \right], \\ (ii) \quad & \frac{d}{dt} \sum_{i=1}^N |v_i|^2 = -\frac{\lambda_1}{N} \sum_{1 \leq i, j \leq N} k_1(x_i, x_j) |v_j - v_i|^2 \\ & \quad + 2I_0 \sum_{i=1}^N v_i \cdot (u_\infty \hat{e}_s - v_i)(1 - \varphi(\zeta_i; \zeta_{cr})), \\ (iii) \quad & \frac{d}{dt} \sum_{i=1}^N \zeta_i = I_0 \sum_{i=1}^N \varphi(\zeta_i; \zeta_{cp}).\end{aligned}$$

Proof. (i) We use the symmetry of the kernel k_1 ($k_1(x_i, x_j) = k_1(x_j, x_i)$) to see

$$\begin{aligned}\frac{d}{dt} \sum_{i=1}^N v_i &= \frac{\lambda_1}{N} \sum_{1 \leq i, j \leq N} k_1(x_j, x_i)(v_j - v_i) + I_0 \left[\sum_{i=1}^N (u_\infty \hat{e}_s - v_i)(1 - \varphi(\zeta_i; \zeta_{cr})) \right] \\ &= I_0 \left[\sum_{i=1}^N (u_\infty \hat{e}_s - v_i)(1 - \varphi(\zeta_i; \zeta_{cr})) \right].\end{aligned}$$

(ii) We first note that due to the symmetry of the kernel k_1 , we have

$$\sum_{1 \leq i, j \leq N} k_1(x_i, x_j) v_i \cdot (v_i - v_j) = - \sum_{1 \leq i, j \leq N} k_1(x_i, x_j) v_j \cdot (v_i - v_j).$$

Hence the above identity yields

$$\begin{aligned} & 2 \sum_{1 \leq i, j \leq N} k_1(x_i, x_j) v_i \cdot (v_i - v_j) \\ &= \sum_{1 \leq i, j \leq N} k_1(x_i, x_j) v_i \cdot (v_i - v_j) - \sum_{1 \leq i, j \leq N} k_1(x_i, x_j) v_j \cdot (v_i - v_j), \end{aligned}$$

which implies that

$$\sum_{1 \leq i, j \leq N} k_1(x_i, x_j) v_i \cdot (v_i - v_j) = \frac{1}{2} \sum_{1 \leq i, j \leq N} k_1(x_i, x_j) |v_i - v_j|^2. \quad (9)$$

We use (9) to obtain

$$\begin{aligned} & \frac{d}{dt} \sum_{i=1}^N |v_i|^2 = 2 \sum_{i=1}^N v_i \cdot \frac{dv_i}{dt} \\ &= -\frac{2\lambda_1}{N} \sum_{1 \leq i, j \leq N} k_1(x_i, x_j) v_i \cdot (v_i - v_j) \\ & \quad + 2I_0 \sum_{i=1}^N v_i \cdot (u_\infty \hat{e}_s - v_i) (1 - \varphi(\zeta_i; \zeta_{cr})) \\ &= -\frac{\lambda_1}{N} \sum_{1 \leq i, j \leq N} k_1(x_i, x_j) |v_j - v_i|^2 \\ & \quad + 2I_0 \sum_{i=1}^N v_i \cdot (u_\infty \hat{e}_s - v_i) (1 - \varphi(\zeta_i; \zeta_{cr})). \end{aligned}$$

(iii) Proving this equality is straightforward and hence is omitted for brevity. \square

Remark 4. Note that in the presence of the external light source, the total mass is the only conserved physical quantity unless there is some coincidental balance between the increase in kinetic energy due to the light source and the decrease by the flocking dissipation.

As noticed in [18], if there is no external light source ($I_0 = 0$), and if the excitation ζ_i is ignored, the system (8) will shrink to the velocity of a center of mass asymptotically in time, depending on the interaction rate k_1 . Hence it is convenient to introduce a center of mass coordinate $[x_c(t), v_c(t)]$:

$$x_c(t) := \frac{1}{N} \sum_{j=1}^N x_j(t), \quad v_c(t) := \frac{1}{N} \sum_{j=1}^N v_j(t).$$

Turning back to the system (7) we have variation estimates for these center of mass coordinates.

Proposition 1. *Suppose that $I_0 > 0$, and that all particles are fully excited after a finite time $t_* > 0$, i.e.,*

$$\varphi(\zeta_i; \zeta_{cr}) = 0, \quad i = 1, \dots, N, \quad t \geq t_*.$$

Then $\forall t \geq t_*$, we have

$$(i) |v_c(t) - u_\infty \hat{e}_s| \leq |v_c(t_*) - u_\infty \hat{e}_s| e^{-I_0(t-t_*)},$$

$$(ii) |x_c(t) - (x_c(t_*) + u_\infty \hat{e}_s(t - t_*))| \leq \frac{1}{I_0} |v_c(t_*) - u_\infty \hat{e}_s|.$$

Proof. (i) Since $\varphi(\zeta_i; \zeta_{cr}) = 0$ for $t > t_*$, it then follows from Lemma 3.1 (i) that

$$\frac{d}{dt} \sum_{i=1}^N v_i = I_0 N u_\infty \hat{e}_s - N I_0 v_c(t), \quad t \geq t_*.$$

This yields

$$\frac{d}{dt} v_c(t) + I_0 v_c(t) = I_0 u_\infty \hat{e}_s, \quad t \geq t_*. \quad (10)$$

The solution of (10) is

$$v_c(t) = e^{-I_0(t-t_*)} v_c(t_*) + u_\infty \hat{e}_s (1 - e^{-I_0(t-t_*)}), \quad t \geq t_*.$$

Therefore

$$v_c(t) - u_\infty \hat{e}_s = (v_c(t_*) - u_\infty \hat{e}_s) e^{-I_0(t-t_*)}, \quad t \geq t_*,$$

and the result follows.

(ii) For $t \geq t_*$, we have

$$x_c(t) = x_c(t_*) + \int_{t_*}^t v_c(\tau) d\tau = x_c(t_*) + u_\infty \hat{e}_s (t - t_*) + \int_{t_*}^t (v_c(\tau) - u_\infty \hat{e}_s) d\tau.$$

We use the result in (i) to see

$$\begin{aligned} & |x_c(t) - (x_c(t_*) + u_\infty \hat{e}_s(t - t_*))| \\ & \leq \left| \int_{t_*}^t (v_c(\tau) - u_\infty \hat{e}_s) d\tau \right| \\ & \leq |v_c(t_*) - u_\infty \hat{e}_s| \left| \int_{t_*}^t e^{-I_0(\tau-t_*)} d\tau \right| \leq \frac{1}{I_0} |v_c(t_*) - u_\infty \hat{e}_s|. \end{aligned}$$

□

We conclude this section by establishing the existence of external driven flocking assuming that the system is fully excited. The result is formulated in terms of the auxiliary function which denotes the statistical variance of the particle velocities:

$$\mathcal{V}(t) := \sum_{i=1}^N |v_i(t) - u_\infty \hat{e}_s|^2.$$

Proposition 2. *Let $(x_i(t), v_i(t), \zeta_i(t))$ be the solution of the system (7). Suppose that $I_0 > 0$, and that all particles are fully excited after a finite time $t_* > 0$, i.e.,*

$$\varphi(\zeta; \zeta_{cr}) = 0, \quad i = 1, \dots, N, \quad t \geq t_*.$$

Then $\forall t \geq t_*$, we have

$$(i) \mathcal{V}(t) \leq \mathcal{V}(t_*) \exp(-2I_0(t - t_*)).$$

$$(ii) |x_i(t) - (x_i(t_*) + u_\infty \hat{e}_s(t - t_*))| \leq \frac{\sqrt{\mathcal{V}(t_*)}}{I_0}.$$

Proof. (i) The system (7) implies that

$$\begin{aligned}
& \frac{d}{dt} \sum_{i=1}^N |v_i - u_\infty \hat{e}_s|^2 \\
&= 2 \sum_{i=1}^N (v_i - u_\infty \hat{e}_s) \cdot \frac{dv_i}{dt} \\
&= \frac{2\lambda_1}{N} \sum_{1 \leq i, j \leq N} k_1(x_j, x_i) (v_i - u_\infty \hat{e}_s) \cdot (v_j - v_i) \\
&\quad - 2I_0 \sum_{i=1}^N |v_i - u_\infty \hat{e}_s|^2 (1 - \varphi(\zeta_i; \zeta_{cr})) \\
&= \frac{2\lambda_1}{N} \sum_{1 \leq i, j \leq N} k_1(x_j, x_i) v_i \cdot (v_j - v_i) - 2I_0 \sum_{i=1}^N |v_i - u_\infty \hat{e}_s|^2 \\
&= -\frac{\lambda_1}{N} \sum_{1 \leq i, j \leq N} k_1(x_j, x_i) |v_j - v_i|^2 - 2I_0 \sum_{i=1}^N |v_i - u_\infty \hat{e}_s|^2 \\
&\leq -2I_0 \sum_{i=1}^N |v_i - u_\infty \hat{e}_s|^2.
\end{aligned}$$

Hence the following differential inequality holds

$$\frac{d}{dt} \mathcal{V}(t) \leq -2I_0 \mathcal{V}(t), \quad t \geq t_*,$$

and the result of the lemma follows.

(ii) The result (i) implies that $\forall t \geq t_*$ and $i = 1, \dots, N$,

$$|v_i(t) - u_\infty \hat{e}_s| \leq \left(\sum_i |v_i(t) - u_\infty \hat{e}_s|^2 \right)^{1/2} = \sqrt{\mathcal{V}(t)} \leq \sqrt{\mathcal{V}(t_*)} \exp(-I_0(t - t_*)). \quad (11)$$

On the other hand, we have

$$x_i(t) = x_i(t_*) + \int_{t_*}^t v_i(\tau) d\tau = x_i(t_*) + u_\infty \hat{e}_s(t - t_*) + \int_{t_*}^t (v_i(\tau) - u_\infty \hat{e}_s) d\tau.$$

Hence, we have

$$\begin{aligned}
& |x_i(t) - (x_i(t_*) + u_\infty \hat{e}_s(t - t_*))| \\
&\leq \int_{t_*}^t |v_i(\tau) - u_\infty \hat{e}_s| d\tau \\
&\leq \sqrt{\mathcal{V}(t_*)} \int_{t_*}^t e^{-I_0(\tau - t_*)} d\tau \leq \sqrt{\mathcal{V}(t_*)} \int_{t_*}^\infty e^{-I_0(\tau - t_*)} d\tau \\
&= \frac{\sqrt{\mathcal{V}(t_*)}}{I_0}.
\end{aligned}$$

□

Remark 5. The flocking result is valid under the assumption that all particles are fully excited. This result is indeed intuitive, since in the regime where all particles are excited, the expected behavior is precisely what we proved, that is that asymptotically, all particles move with an identical velocity towards the light source. The interesting regime in which some particles are sufficiently excited to initiate a motion while other particles remain stationary is not covered by the flocking result.

Remark 6. As can be seen in the proof, when the light source is turned on, the explicit form of k_1 is not important as long as it satisfies the condition (3).

3.3. On the growth of the excitation level. In our previous propositions we assumed that the particles are fully excited after a finite time. While this may sound like a severe constraint, it turns out to be the generic case as discussed in this section.

Recall that the equation for excitation level ζ_i (see (7)) is

$$\frac{d\zeta_i}{dt} = \frac{\lambda_2}{N} \sum_{l=1}^N k_2(x_l, x_i)(\zeta_l - \zeta_i) + I_0 \varphi(\zeta_i; \zeta_{cp}). \quad (12)$$

Here ζ_{cp} is the capacity of the excitation and $\varphi(\zeta_i; \zeta_{cp})$ is a smooth cut-off function that is defined as

$$\varphi(\zeta_i; \zeta_{cp}) = \begin{cases} 1, & \zeta_i \leq \zeta_{cp}, \\ 0, & \zeta_i > 2\zeta_{cp}. \end{cases} \quad 0 \leq \varphi \leq 1.$$

We would like to argue that the excitation ζ_i asymptotically approaches a constant value that is greater than the value of $2\zeta_{cp}$ independently of the particle number i . We will refer to that asymptotic value as the “flocking phase value”. Without loss of generality, we may assume that all particles are initially below the level ζ_{cp} , i.e.,

$$\zeta_i(0) < \zeta_{cp}.$$

In fact, the dynamics of ζ_i undergoes three distinct phases (initial growth phase, transition phase and flocking) before it is finally approaches the flocking phase value. After the initial growth phase, the particles are already fully excited, i.e., $\varphi(\zeta_i; \zeta_{cp}) = 0$ (assuming $2\zeta_{cp} \leq \zeta_{cp}$).

1. **The initial growth phase.** To study this phase we assume the following:

(a) The critical threshold and capacity for excitation satisfy

$$2\zeta_{cr} \leq \zeta_{cp}.$$

(b) The interaction rate k_2 is nonnegative and bounded, i.e.,

$$0 \leq k_2(x_l, x_i) \leq \|k_2\|_{L^\infty} < \infty.$$

(c) I_0, ζ_{cp} , and λ_2 satisfy the condition

$$I_0 - 2\|k_2\|_{L^\infty} \lambda_2 \zeta_{cp} > 0.$$

In this initial growth phase ($\zeta_i \leq \zeta_{cp}$), we have

$$\frac{\lambda_2}{N} \sum_{l=1}^N k_2(x_l, x_i)(\zeta_l - \zeta_i) \geq -2\lambda_2 \|k_2\|_{L^\infty} \zeta_{cp},$$

which yields

$$\frac{d\zeta_i}{dt} \geq -2\lambda_2 \|k_2\|_{L^\infty} \zeta_{cp} + I_0.$$

Hence we have

$$\zeta_i(t) \geq \zeta_i(0) + (I_0 - 2\lambda_2 \|k_2\|_{L^\infty} \zeta_{cp})t. \quad (13)$$

Let t_*^i be the first time when the RHS of (13) exceeds ζ_{cp} and set

$$t_* := \min_{1 \leq i \leq N} t_*^i.$$

Note that after initial growth phase $t > t_*^1$, the dynamics of particles in (x_i, v_i) becomes decoupled from the equation of ζ_i , hence, at this stage, the excitation level is irrelevant to the dynamics.

2. **The transition phase.** This dynamics in this phase is complicated due to the relative competition between flocking dissipation and external forcing. What happens during that phase is interesting, but it is unrelated to the asymptotic behavior of the particles and we therefore do not study it here.
3. **The final flocking phase.** In this phase, the excitation level of all particles exceeds the value of $2\zeta_{cp}$. Hence, the dynamics of the excitation satisfies

$$\frac{d\zeta_i}{dt} = \frac{\lambda_2}{N} \sum_{l=1}^N k_2(x_l, x_i)(\zeta_l - \zeta_i), \quad t \geq t^*,$$

where t^* is the time when excitations of all particles exceed the value $2\zeta_{cp}$. In this case, the standard Cucker-Smale's flocking analysis shows that ζ_i converges to the flocking value $\frac{1}{N} \sum_{j=1}^N \zeta_j(t^*)$ exponentially fast under the suitable ansatz (5) for k_2 with $\beta \leq 1/2$ (see [15, 16, 18]), i.e.,

$$\lim_{t \rightarrow \infty} \max_{i=1, \dots, N} \left| \zeta_i(t) - \frac{1}{N} \sum_{j=1}^N \zeta_j(t^*) \right| = 0,$$

and this convergence is exponentially fast.

Remark 7. Our definition of the excitation capacity, ζ_{cp} , should not be interpreted as the maximal excitation value. Indeed, ζ may (and will eventually) exceed ζ_{cp} . In our context, by ‘‘capacity’’ we refer to the level of excitation in which it starts saturating. The asymptotic value is about $2\zeta_{cp}$.

3.4. Numerical simulations. In this section we present results of numerical simulations of the system (7). In all simulations we used $N = 100$ particles. Their initial locations were drawn from a uniform distribution in the domain $[0, 100]^2$. Their initial velocities were also uniformly distributed in $[0, 100]^2$. The internal flocking behavior thus amounts to a convergence to the average velocity, i.e., $v = (50, 50)$. The initial excitation for all particles were uniformly distributed in $[0, 0.001]$. Both kernels, k_1 and k_2 in (7) were chosen as

$$k_1(x_j, x_i) = k_2(x_j, x_i) = \frac{1}{(1 + |x_j - x_i|^2)^\beta}, \quad 1 \leq i, j \leq 100,$$

with $\beta = 0.25$, a value for which internal flocking is known to emerge. An external forcing was used with a velocity that was set as $u_\infty = (60, 0)$, and a magnitude $I_0 = 0.1$ in one experiment and $I_0 = 10$ in a second experiment. In both cases we chose $\lambda_1 = \lambda_2 = 100$. The critical value of the excitation was taken as $\zeta_{cr} = 0.3$, while ζ_{cp} was set as $2\zeta_{cr}$.

Our results shows that one should expect in both cases to see an exponential convergence of the velocities of all particles to the velocity dictated by the external forcing, i.e., $(60, 0)$. Figure 4 shows how the velocity of all particles changes over

time (for $I_0 = 0.1$). The change of the velocity profile over time for one particle ($I_0 = 0.1$) is shown in Figure 5. A similar plots for $I_0 = 10$ are shown in Figure 6 (Note the different time-scales in this case). Indeed, as expected, the asymptotic velocities of all particles in all cases is the one that is dictated by the external forcing, i.e., we see an exponential convergence of the velocity field to $(60, 0)$. The difference between these two examples has to do with the relative strengths of the internal flocking and the external forcing. When $\lambda_1 = 100$ and $I_0 = 0.1$, it takes more time for the excitation to grow and reach its critical value, after which the external forcing becomes the dominant one in the velocity equation. Before this happens, the internal flocking mechanism is more dominant, and the velocity of the particles converges to the averaged initial velocity.

Only after sufficient excitation has been built, the external forcing becomes dominant. We demonstrate how the excitation changes for a single particle in Figure 7. As opposed to this case, an accelerated convergence towards the value that is dictated by the external forcing can be seen when $I_0 = 10$. Even then, there is a delayed motion phase that takes place until all particles have started aligning their motion based on the external forcing.

4. A kinetic model for phototaxis. In this section we present a collisional kinetic model for the one-particle distribution function with an internal variable denoting a nonnegative excitation level. Similarly to the derivation of the Boltzmann equation and Vlasov-type equations [4, 13, 18, 35, 36], we derive a kinetic model starting from the Liouville equation. We then make use of the Bogoliubov-Born-Green-Kirkwood-Yvon (BBGKY) hierarchy and the assumption of molecular chaos to derive a Vlasov-type equation. Finally we add the collision effect between the particles and the medium where they move.

4.1. A formal derivation of a Vlasov-type model. In this part, we present a Vlasov-type equation modeling the collective behavior of N -particle system. For the time being, we ignore the collisions between particle and background medium. Our approach follows from the standard BBGKY hierarchy and a molecular chaos assumption to close the hierarchy. The rigorous justification of the molecular chaos assumption is very difficult, and is beyond the scope of this paper.

Let $f^N = f^N(x_1, v_1, \zeta_1, \dots, x_N, v_N, \zeta_N, t)$ be the probability density function (N -particle distribution function) of particles in N -particle phase space-excitation-time $(\mathbb{R}^{2d} \times \mathbb{R}_+)^N \times \mathbb{R}$. Since the particles are indistinguishable, f^N is symmetric in its argument, i.e., for $1 \leq i, j \leq N$,

$$f^N(\dots, x_i, v_i, \zeta_j, \dots, x_j, v_j, \zeta_j, \dots, t) = f^N(\dots, x_j, v_j, \zeta_j, \dots, x_i, v_i, \zeta_i, \dots, t). \quad (14)$$

Then f^N satisfies the Liouville equation [23, 26]:

$$\frac{\partial f^N}{\partial t} = - \sum_{i=1}^N \operatorname{div}_{x_i} \left(\frac{dx_i}{dt} f^N \right) - \sum_{i=1}^N \operatorname{div}_{v_i} \left(\frac{dv_i}{dt} f^N \right) - \sum_{i=1}^N \frac{\partial}{\partial \zeta_i} \left(\frac{d\zeta_i}{dt} f^N \right),$$

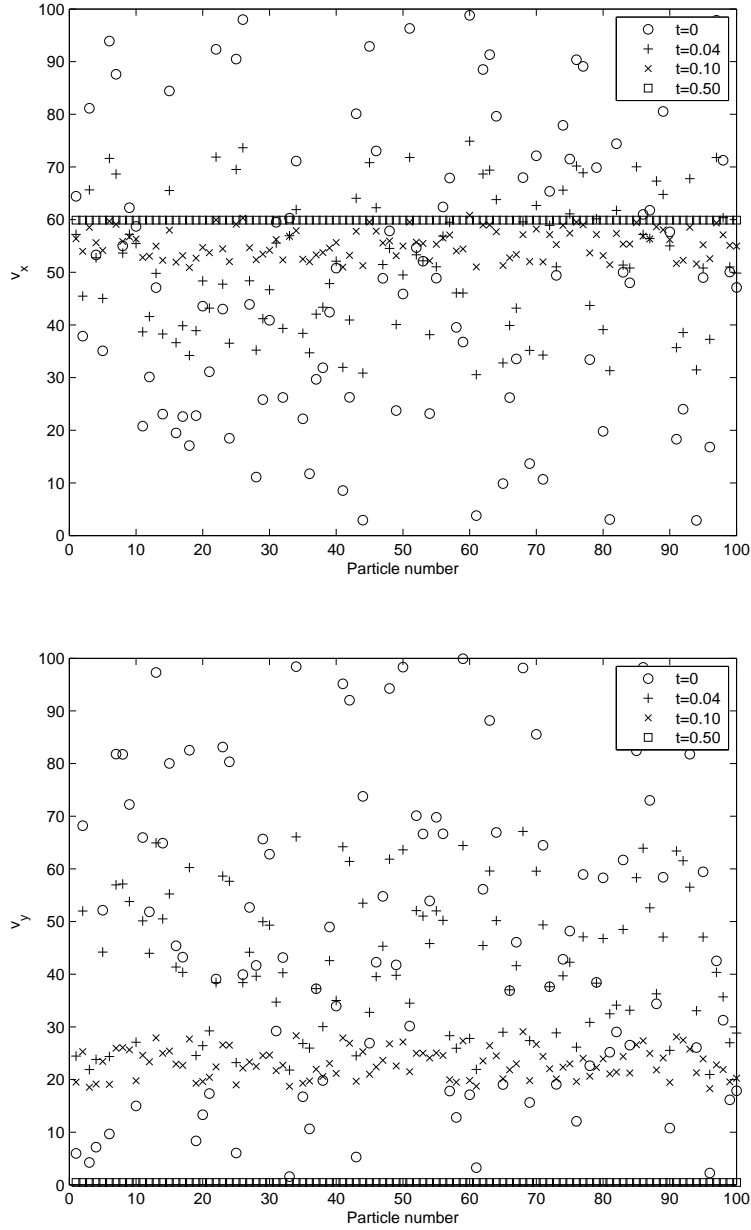


FIGURE 4. The change in the velocity profile of all 100 particles over time. $I_0 = 0.1$, $\lambda_i = 100$, $i = 1, 2$. (upper) the velocity component in the x direction. (lower) the velocity component in the y direction.

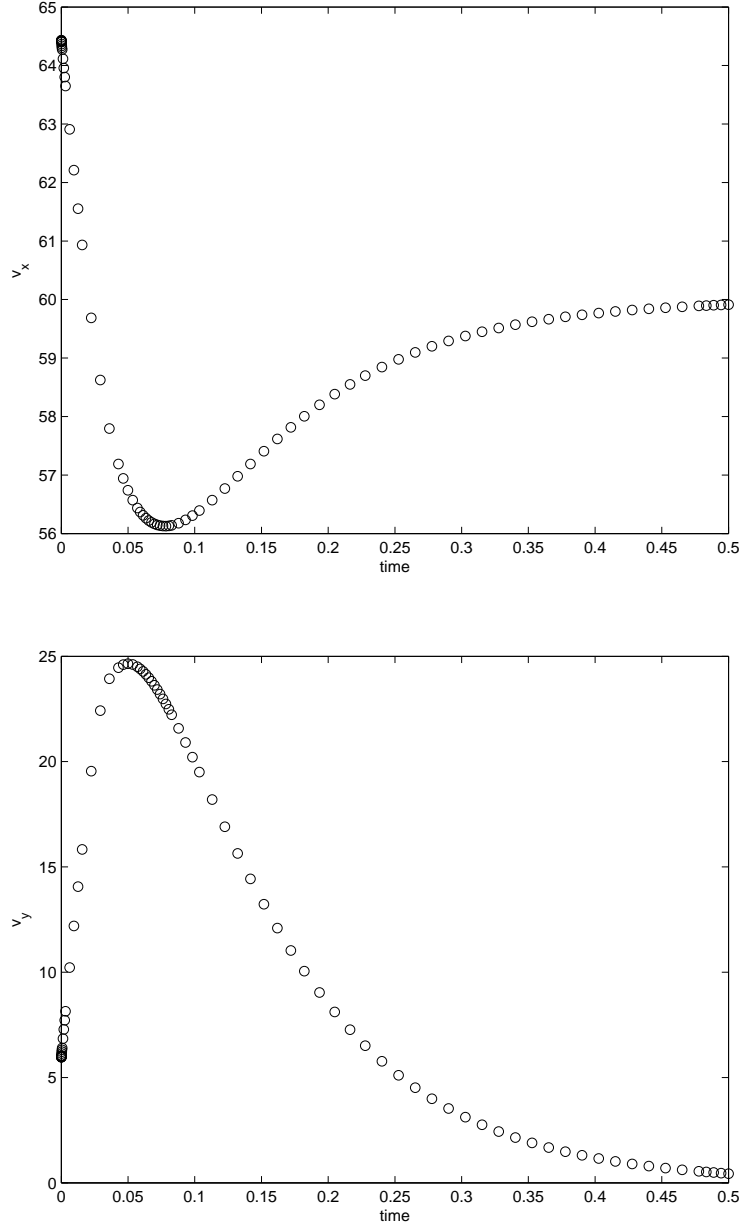


FIGURE 5. The change in the velocity profile of one particle over time. $I_0 = 0.1$, $\lambda_i = 100$, $i = 1, 2$. (upper) the velocity component in the x direction. (lower) the velocity component in the y direction.

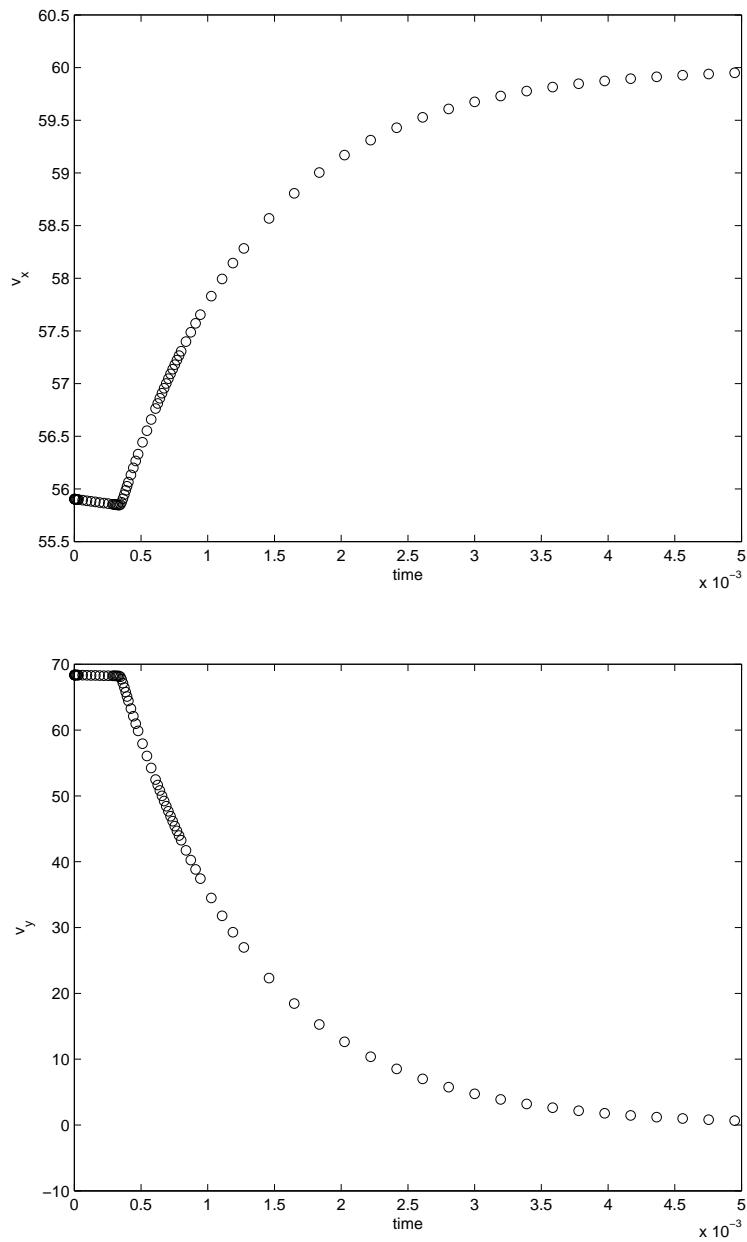


FIGURE 6. The change in the velocity profile of one particle over time. $I_0 = 10$, $\lambda_i = 100$, $i = 1, 2$. (upper) the velocity component in the x direction. (lower) the velocity component in the y direction.

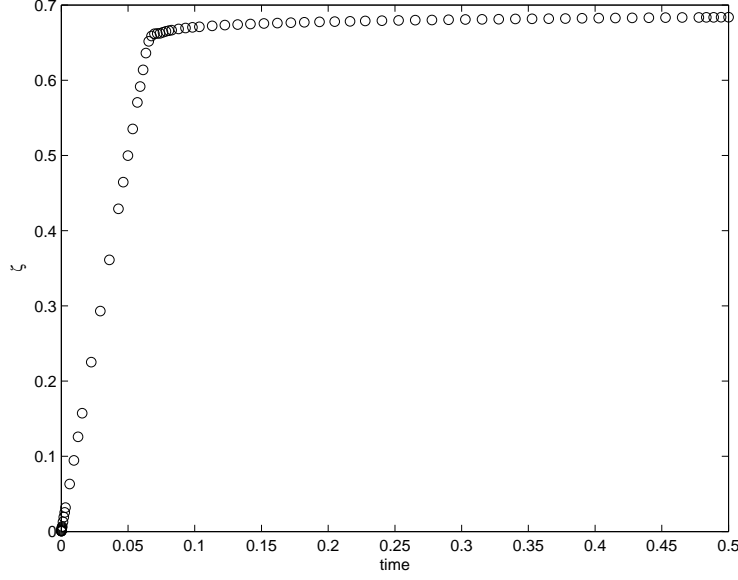


FIGURE 7. The change in the value of the excitation of one particle.
 $I_0 = 0.1$, $\lambda_i = 100$, $i = 1, 2$.

which in view of the particle system (7) becomes

$$\begin{aligned}
\partial_t f^N &= - \sum_{i=1}^N \operatorname{div}_{x_i} (v_i f^N) \\
&\quad - \sum_{i=1}^N \operatorname{div}_{v_i} \left[\left(\frac{\lambda_1}{N} \sum_{k=1}^N k_1(x_k, x_i) (v_k - v_i) + I_0 (u_\infty \hat{e}_s - v_i) (1 - \varphi(\zeta_i; \zeta_{cr})) \right) f^N \right] \\
&\quad - \sum_{i=1}^N \partial_{\zeta_i} \left[\left(\frac{\lambda_2}{N} \sum_{k=1}^N k_2(x_k, x_i) (\zeta_k - \zeta_i) + I_0 \varphi(\zeta_i; \zeta_{cp}) \right) f^N \right] \\
&=: -\mathcal{I}_1 - \mathcal{I}_2 - \mathcal{I}_3.
\end{aligned} \tag{15}$$

We now introduce a j -particle distribution function f_j^N which is a marginal distribution function of f^N : For $1 \leq j \leq N-1$,

$$f_j^N(x_1, v_1, \zeta_1, \dots, x_j, v_j, \zeta_j, t) \equiv \int_{\mathbb{R}^{2d(N-j)} \times \mathbb{R}_+^{N-j}} f^N d\Sigma_{j+1}^N. \tag{16}$$

Here we used a simplified notation $d\Sigma_{j+1}^N \equiv dx_{j+1} dv_{j+1} d\zeta_{j+1} \cdots dx_N dv_N d\zeta_N$, and integrate (15) with respect to $d\Sigma_{j+1}^N$. This results with the three integrals of the divergence terms in (15). For notational simplicity, we suppress the t -dependence in f_j^N , i.e.,

$$f_j^N(x_1, v_1, \zeta_1, \dots, x_j, v_j, \zeta_j) \equiv f_j^N(x_1, v_1, \zeta_1, \dots, x_j, v_j, \zeta_j, t).$$

Lemma 4.1. *Assume that f^N vanishes at infinity in the N -particle phase (+ excitation) space. Then the following equalities hold:*

$$\begin{aligned}
(i) \quad & \int_{\mathbb{R}^{2d(N-j)} \times \mathbb{R}_+^{N-j}} \mathcal{I}_1 d\Sigma_{j+1}^N = \sum_{i=1}^j \operatorname{div}_{x_i} (v_i f_j^N). \\
(ii) \quad & \int_{\mathbb{R}^{2d(N-j)} \times \mathbb{R}_+^{N-j}} \mathcal{I}_2 d\Sigma_{j+1}^N \\
&= \sum_{i=1}^j \operatorname{div}_{v_i} \left[I_0 (u_\infty \hat{e}_s - v_i) (1 - \varphi(\zeta_i; \zeta_{cr})) f_j^N \right] \\
&+ \frac{\lambda_1}{N} \sum_{i=1}^j \sum_{k=1}^j k_1(x_k, x_i) \operatorname{div}_{v_i} \left[(v_k - v_i) f_j^N \right] \\
&+ \frac{\lambda_1}{N} (N-j) \sum_{i=1}^j \operatorname{div}_{v_i} \\
&\quad \left[\int_{\mathbb{R}^{2d}} k_1(x_{j+1}, x_i) (v_{j+1} - v_i) f_{j+1}^N dx_{j+1} dv_{j+1} d\zeta_{j+1} \right]. \\
(iii) \quad & \int_{\mathbb{R}^{2d(N-j)} \times \mathbb{R}_+^{N-j}} \mathcal{I}_3 d\Sigma_{j+1}^N \\
&= \sum_{i=1}^j \partial_{\zeta_i} \left[I_0 \varphi(\zeta_i; \zeta_{cp}) f_j^N \right] + \frac{\lambda_2}{N} \sum_{i=1}^j \sum_{k=1}^j k_2(x_k, x_i) \partial_{\zeta_i} \left[(\zeta_k - \zeta_i) f_j^N \right] \\
&+ \frac{\lambda_2}{N} (N-j) \sum_{i=1}^j \partial_{\zeta_i} \\
&\quad \left[\int_{\mathbb{R}^{2d}} k_2(x_{j+1}, x_i) (\zeta_{j+1} - \zeta_i) f_{j+1}^N dx_{j+1} dv_{j+1} d\zeta_{j+1} \right].
\end{aligned}$$

Proof. (i) Note that

$$\begin{aligned}
& \int_{\mathbb{R}^{2d(N-j)} \times \mathbb{R}_+^{N-j}} \mathcal{I}_1 d\Sigma_{j+1}^N \\
&= \sum_{i=1}^j \int_{\mathbb{R}^{2d(N-j)} \times \mathbb{R}_+^{N-j}} \operatorname{div}_{x_i} (v_i f_j^N) d\Sigma_{j+1}^N \\
&\quad + \sum_{i=j+1}^N \int_{\mathbb{R}^{2d(N-j)} \times \mathbb{R}_+^{N-j}} \operatorname{div}_{x_i} (v_i f_j^N) d\Sigma_{j+1}^N \\
&= \sum_{i=1}^j \operatorname{div}_{x_i} (v_i f_j^N).
\end{aligned}$$

(ii) The force term can be treated as follows.

$$\begin{aligned}
& \int_{\mathbb{R}^{2d(N-j)} \times \mathbb{R}_+^{N-j}} \mathcal{I}_2 d\Sigma_{j+1}^N \\
&= \sum_{i=1}^j \int_{\mathbb{R}^{2d(N-j)} \times \mathbb{R}_+^{N-j}} \operatorname{div}_{v_i} \left[\left(\frac{\lambda_1}{N} \sum_{k=1}^j k_1(x_k, x_i)(v_k - v_i) \right. \right. \\
&\quad \left. \left. + I_0(u_\infty \hat{e}_s - v_i)(1 - \varphi(\zeta_i; \zeta_{cr})) \right) f^N \right] d\Sigma_{j+1}^N \\
&\quad + \sum_{i=1}^j \int_{\mathbb{R}^{2d(N-j)} \times \mathbb{R}_+^{N-j}} \operatorname{div}_{v_i} \left[\frac{\lambda_1}{N} \sum_{k=j+1}^N k_1(x_k, x_i)(v_k - v_i) f^N \right] d\Sigma_{j+1}^N \\
&\quad + \sum_{i=j+1}^N \int_{\mathbb{R}^{2d(N-j)} \times \mathbb{R}_+^{N-j}} \operatorname{div}_{v_i} \left[\left(\frac{\lambda_1}{N} \sum_{k=1}^N k_1(x_k, x_i)(v_k - v_i) \right. \right. \\
&\quad \left. \left. + I_0(u_\infty \hat{e}_s - v_i)(1 - \varphi(\zeta_i; \zeta_{cr})) \right) f^N \right] d\Sigma_{j+1}^N \\
&=: \int_{\mathbb{R}^{2d(N-j)} \times \mathbb{R}_+^{N-j}} (\mathcal{I}_2^1 + \mathcal{I}_2^2 + \mathcal{I}_2^3) d\Sigma_{j+1}^N.
\end{aligned}$$

Each term can be treated as follows.

- Case 1:

$$\begin{aligned}
& \int_{\mathbb{R}^{2d(N-j)} \times \mathbb{R}_+^{N-j}} \mathcal{I}_2^1 d\Sigma_{j+1}^N \\
&= \frac{\lambda_1}{N} \sum_{i=1}^j \sum_{k=1}^j k_1(x_k, x_i) \operatorname{div}_{v_i} \left[(v_i - v_k) f_j^N \right] \\
&\quad + \sum_{i=1}^j \operatorname{div}_{v_i} \left(I_0(u_\infty \hat{e}_s - v_i)(1 - \varphi(\zeta_i; \zeta_{cr})) f_j^N \right).
\end{aligned}$$

- Case 2:

$$\begin{aligned}
& \int_{\mathbb{R}^{2d(N-j)} \times \mathbb{R}_+^{N-j}} \mathcal{I}_2^2 d\Sigma_{j+1}^N \\
&= \frac{\lambda_1}{N} \sum_{i=1}^j \int_{\mathbb{R}^{2d(N-j)} \times \mathbb{R}_+^{N-j}} \sum_{k=j+1}^N k_1(x_k, x_i) \operatorname{div}_{v_i} \left[(v_k - v_i) f^N \right] d\Sigma_{j+1}^N.
\end{aligned}$$

Since the particles are indistinguishable, (14) holds, and hence

$$k_1(x_k, x_i) \operatorname{div}_{v_i} \left[(v_k - v_i) f^N \right] = k_1(x_{j+1}, x_i) \operatorname{div}_{v_i} \left[(v_{j+1} - v_i) f^N \right], \quad \forall k \geq j+1.$$

This implies that

$$\begin{aligned}
& \int_{\mathbb{R}^{2d(N-j)} \times \mathbb{R}_+^{N-j}} \mathcal{I}_2^2 d\Sigma_{j+1}^N \\
&= \frac{\lambda_1}{N} (N-j) \sum_{i=1}^j \int_{\mathbb{R}^{2d(N-j)} \times \mathbb{R}_+^{N-j}} k_1(x_{j+1}, x_i) \operatorname{div}_{v_i} \left[(v_{j+1} - v_i) f^N \right] d\Sigma_{j+1}^N.
\end{aligned}$$

Finally, we note that $d\Sigma_{j+1}^N = dx_{j+1}dv_{j+1}d\zeta_{j+1}d\Sigma_{j+2}^N$, so that integrating with respect to Σ_{j+2}^N results with

$$\begin{aligned} & \int_{\mathbb{R}^{2d(N-j)} \times \mathbb{R}_+^{N-j}} \mathcal{I}_2^2 d\Sigma_{j+1}^N \\ &= \frac{\lambda_1}{N} (N-j) \sum_{i=1}^j \operatorname{div}_{v_i} \left[\int_{\mathbb{R}^{2d} \times \mathbb{R}_+} k_1(x_{j+1}, x_i) (v_{j+1} - v_i) f_{j+1}^N dx_{j+1} dv_{j+1} d\zeta_{j+1} \right]. \end{aligned}$$

• Case 3:

$$\begin{aligned} & \int_{\mathbb{R}^{2d(N-j)} \times \mathbb{R}_+^{N-j}} \mathcal{I}_2^3 d\Sigma_{j+1}^N \\ &= \frac{\lambda_1}{N} \sum_{i=j+1}^N \sum_{k=1}^N \int_{\mathbb{R}^{2d(N-j)} \times \mathbb{R}_+^{N-j}} k_1(x_k, x_i) \operatorname{div}_{v_i} [(v_k - v_i) f^N] d\Sigma_{j+1}^N \quad (17) \\ &+ \sum_{i=j+1}^N \int_{\mathbb{R}^{2d(N-j)} \times \mathbb{R}_+^{N-j}} I_0 \operatorname{div}_{v_i} [(u_\infty \hat{e}_s - v_i) (1 - \varphi(\zeta_i; \zeta_{cp})) f^N] d\Sigma_{j+1}^N. \end{aligned}$$

Using the divergence theorem, the RHS of (17) vanishes, which concludes case 3. All that is left is to combine Cases 1–3 to obtain the result of part (ii) of the Lemma. (iii) The excitation term is treated in a similar way.

$$\begin{aligned} & \int_{\mathbb{R}^{2d(N-j)} \times \mathbb{R}_+^{N-j}} \mathcal{I}_3 d\Sigma_{j+1}^N \\ &= \sum_{i=1}^j \int_{\mathbb{R}^{2d(N-j)} \times \mathbb{R}_+^{N-j}} \partial_{\zeta_i} \left[\left(\frac{\lambda_2}{N} \sum_{k=1}^j k_2(x_k, x_i) (\zeta_k - \zeta_i) + I_0 \varphi(\zeta_i; \zeta_{cp}) \right) f^N \right] d\Sigma_{j+1}^N \\ &+ \sum_{i=1}^j \int_{\mathbb{R}^{2d(N-j)} \times \mathbb{R}_+^{N-j}} \partial_{\zeta_i} \left[\frac{\lambda_2}{N} \sum_{k=j+1}^N k_2(x_k, x_i) (\zeta_k - \zeta_i) f^N \right] d\Sigma_{j+1}^N \\ &+ \sum_{i=j+1}^N \int_{\mathbb{R}^{2d(N-j)} \times \mathbb{R}_+^{N-j}} \partial_{\zeta_i} \left[\left(\frac{\lambda_2}{N} \sum_{k=1}^N k_2(x_k, x_i) (\zeta_k - \zeta_i) + I_0 \varphi(\zeta_i; \zeta_{cp}) \right) f^N \right] d\Sigma_{j+1}^N \\ &=: \int_{\mathbb{R}^{2d(N-j)} \times \mathbb{R}_+^{N-j}} (\mathcal{I}_3^1 + \mathcal{I}_3^2 + \mathcal{I}_3^3) d\Sigma_{j+1}^N. \end{aligned}$$

- Case 1:

$$\begin{aligned}
& \int_{\mathbb{R}^{2d(N-j)} \times \mathbb{R}_+^{N-j}} \mathcal{I}_3^1 d\Sigma_{j+1}^N \\
&= \sum_{i=1}^j \partial_{\zeta_i} \left[\left(\frac{\lambda_2}{N} \sum_{k=1}^j k_2(x_k, x_i) (\zeta_k - \zeta_i) + I_0 \varphi(\zeta_i; \zeta_{cp}) \right) \right. \\
&\quad \left. \int_{\mathbb{R}^{2d(N-j)} \times \mathbb{R}_+^{N-j}} f^N d\Sigma_{j+1}^N \right] \\
&= \frac{\lambda_2}{N} \sum_{i=1}^j \sum_{k=1}^j k_2(x_k, x_i) \partial_{\zeta_i} [(\zeta_k - \zeta_i) f_j^N] + \sum_{i=1}^j I_0 \partial_{\zeta_i} [\varphi(\zeta_i; \zeta_{cp}) f_j^N].
\end{aligned}$$

- Case 2: once again we make use of the particles being indistinguishable.

$$\begin{aligned}
& \int_{\mathbb{R}^{2d(N-j)} \times \mathbb{R}_+^{N-j}} \mathcal{I}_3^2 d\Sigma_{j+1}^N \\
&= \frac{\lambda_2}{N} \sum_{i=1}^j \int_{\mathbb{R}^{2d(N-j)} \times \mathbb{R}_+^{N-j}} \sum_{k=j+1}^N k_2(x_k, x_i) \partial_{\zeta_i} [(\zeta_k - \zeta_i) f^N] d\Sigma_{j+1}^N \\
&= \frac{\lambda_2}{N} (N-j) \sum_{i=1}^j \int_{\mathbb{R}^{2d(N-j)} \times \mathbb{R}_+^{N-j}} k_2 a(x_{j+1}, x_i) \partial_{\zeta_i} [(\zeta_{j+1} - \zeta_i) f^N] d\Sigma_{j+1}^N \\
&= \frac{\lambda_2}{N} (N-j) \sum_{i=1}^j \partial_{\zeta_i} \left[\int_{\mathbb{R}^{2d} \times \mathbb{R}_+} k_2(x_{j+1}, x_i) \right. \\
&\quad \left. (\zeta_{j+1} - \zeta_i) f_{j+1}^N dx_{j+1} dv_{j+1} d\zeta_{j+1} \right].
\end{aligned}$$

- Case 3:

$$\begin{aligned}
& \int_{\mathbb{R}^{2d(N-j)} \times \mathbb{R}_+^{N-j}} \mathcal{I}_3^3 d\Sigma_{j+1}^N \\
&= \frac{\lambda_2}{N} \sum_{i=j+1}^N \sum_{k=1}^N \int_{\mathbb{R}^{2d(N-j)} \times \mathbb{R}_+^{N-j}} k_2(x_k, x_i) \partial_{\zeta_i} [(\zeta_k - \zeta_i) f^N] d\Sigma_{j+1}^N \\
&\quad + \sum_{i=j+1}^N \int_{\mathbb{R}^{2d(N-j)} \times \mathbb{R}_+^{N-j}} I_0 \partial_{\zeta_i} [\varphi(\zeta_i; \zeta_{cp}) f^N] d\Sigma_{j+1}^N = 0.
\end{aligned}$$

Combining Cases 1–3 concludes proving part (iii) of the Lemma. \square

The hierarchy for the j -particle density function, f_j^N , can now be obtained by combining (15), (16), and Lemma 4.1:

$$\begin{aligned}
& \partial_t f_j^N + \sum_{i=1}^j \operatorname{div}_{x_i}(v_i f_j^N) + \sum_{i=1}^j \operatorname{div}_{v_i} \left[I_0(u_\infty \hat{e}_s - v_i)(1 - \varphi(\zeta_i; \zeta_{cr})) f_j^N \right] \\
& \quad + \sum_{i=1}^j \partial_{\zeta_i} \left[I_0 \varphi(\zeta_i; \zeta_{cp}) f_j^N \right] \\
& = -\frac{\lambda_1}{N} \sum_{i=1}^j \sum_{k=1}^j k_2(x_k, x_i) \operatorname{div}_{v_i} \left[(v_k - v_i) f_j^N \right] \\
& \quad - \frac{\lambda_2}{N} \sum_{i=1}^j \sum_{k=1}^j k_2(x_k, x_i) \partial_{\zeta_i} \left[(\zeta_k - \zeta_i) f_j^N \right] \\
& \quad - \frac{\lambda_1}{N} (N-j) \sum_{i=1}^j \operatorname{div}_{v_i} \left[\int_{\mathbb{R}^{2d} \times \mathbb{R}_+} k_1(x_{j+1}, x_i) (v_{j+1} - v_i) f_{j+1}^N dx_{j+1} dv_{j+1} d\zeta_{j+1} \right] \\
& \quad - \frac{\lambda_2}{N} (N-j) \sum_{i=1}^j \partial_{\zeta_i} \left[\int_{\mathbb{R}^{2d} \times \mathbb{R}_+} k_2(x_{j+1}, x_i) (\zeta_{j+1} - \zeta_i) f_{j+1}^N dx_{j+1} dv_{j+1} d\zeta_{j+1} \right].
\end{aligned}$$

As in the Boltzmann-Grad's limit for the Boltzmann equation, we take the mean field limit $N \rightarrow \infty$, and we set $\lim_{N \rightarrow \infty} f_j^N = f_j$ to find

$$\begin{aligned}
& \partial_t f_j + \sum_{i=1}^j \operatorname{div}_{x_i}(v_i f_j) + \sum_{i=1}^j \operatorname{div}_{v_i} \left[I_0(u_\infty \hat{e}_s - v_i)(1 - \varphi(\zeta_i; \zeta_{cr})) f_j \right] \\
& \quad + \sum_{i=1}^j \partial_{\zeta_i} \left[I_0 \varphi(\zeta_i; \zeta_{cp}) f_j \right] \\
& = -\lambda_1 \sum_{i=1}^j \operatorname{div}_{v_i} \left[\int_{\mathbb{R}^{2d} \times \mathbb{R}_+} k_1(x_{j+1}, x_i) (v_{j+1} - v_i) f_{j+1} dx_{j+1} dv_{j+1} d\zeta_{j+1} \right] \\
& \quad - \lambda_2 \sum_{i=1}^j \partial_{\zeta_i} \left[\int_{\mathbb{R}^{2d} \times \mathbb{R}_+} k_2(x_{j+1}, x_i) (\zeta_{j+1} - \zeta_i) f_{j+1} dx_{j+1} dv_{j+1} d\zeta_{j+1} \right].
\end{aligned} \tag{18}$$

In particular, when $j = 1$, (18) implies that

$$\begin{aligned}
& \partial_t f_1 + \operatorname{div}_{x_1}(v_1 f_1) + \operatorname{div}_{v_1} \left[I_0(u_\infty \hat{e}_s - v_1)(1 - \varphi(\zeta_1; \zeta_{cr})) f_1 \right. \\
& \quad \left. + \lambda_1 \int_{\mathbb{R}^{2d} \times \mathbb{R}_+} k_1(x_2, x_1) (v_2 - v_1) f_2 dx_2 dv_2 d\zeta_2 \right] \\
& \quad + \partial_{\zeta_1} \left[I_0 \varphi(\zeta_1; \zeta_{cp}) f_1 + \lambda_2 \int_{\mathbb{R}^{2d} \times \mathbb{R}_+} k_2(x_2, x_1) (\zeta_2 - \zeta_1) f_2 dx_2 dv_2 d\zeta_2 \right] = 0.
\end{aligned} \tag{19}$$

In order to close the hierarchy in (19), we employ the so called ‘‘molecular chaos’’ assumption for the two-point particle distribution function:

$$f_2(x_1, v_1, \zeta_1, x_2, v_2, \zeta_2, t) = f_1(x_1, v_1, t; \zeta_1) f_1(x_2, v_2, t; \zeta_2). \tag{20}$$

Under the molecular chaos assumption (20), the one particle distribution function $f := f_1$ satisfies the Vlasov-type mean field equation:

$$\begin{aligned} \partial_t f + \operatorname{div}_x(vf) + \operatorname{div}_v \left[I_0(u_\infty \hat{e}_s - v)(1 - \varphi(\zeta; \zeta_{cr}))f + \lambda_1 K_1[f]f \right] \\ + \partial_\zeta \left[I_0 \varphi(\zeta; \zeta_{cp})f + \lambda_2 K_2[f]f \right] = 0, \end{aligned} \quad (21)$$

where $x := x_1$, $v := v_1$, $\zeta := \zeta_1$, and the kernels are given by

$$\begin{aligned} K_1[f](x, v, t) &:= - \int_{\mathbb{R}^{2d} \times \mathbb{R}_+} k_1(x, y)(v - v_*)f(y, v_*, t; \zeta_*) dy dv_* d\zeta_*, \\ K_2[f](x, \zeta, t) &:= - \int_{\mathbb{R}^{2d} \times \mathbb{R}_+} k_2(x, y)(\zeta - \zeta_*)f(y, v_*, t; \zeta_*) dy dv_* d\zeta_*. \end{aligned} \quad (22)$$

Remark 8. The notation used in (20), $f(x, v, t; \zeta)$, is chosen as to distinguish between the role of the excitation as an “internal” parameter, and the role of other variables.

It turns out that the Vlasov-type kinetic model (21) has a flocking mechanism which we will now study. Define a functional \mathcal{F} that is associated with f :

$$\mathcal{F}(f(t)) := \int_{\mathbb{R}^{2d} \times \mathbb{R}_+} |v - u_\infty \hat{e}_s|^2 f(x, v, t; \zeta) d\zeta dv dx.$$

According to (21), the time derivative of $\mathcal{F}(f(t))$ is

$$\begin{aligned} \frac{d}{dt} \mathcal{F}(f(t)) &= \int_{\mathbb{R}^{2d} \times \mathbb{R}_+} |v - u_\infty \hat{e}_s|^2 \partial_t f(x, v, t; \zeta) d\zeta dv dx \\ &= - \int_{\mathbb{R}^{2d} \times \mathbb{R}_+} |v - u_\infty \hat{e}_s|^2 \operatorname{div}_x(vf) d\zeta dv dx \\ &\quad - \int_{\mathbb{R}^{2d} \times \mathbb{R}_+} |v - u_\infty \hat{e}_s|^2 \\ &\quad \quad \operatorname{div}_v \left[\lambda_1 K_1[f]f + I_0(u_\infty \hat{e}_s - v)(1 - \varphi(\zeta; \zeta_{cr}))f \right] d\zeta dv dx \\ &\quad - \int_{\mathbb{R}^{2d} \times \mathbb{R}_+} |v - u_\infty \hat{e}_s|^2 \partial_\zeta \left[\lambda_2 K_2[f]f + I_0 \varphi(\zeta; \zeta_{cp})f \right] d\zeta dv dx \\ &:= \mathcal{J}_1 + \mathcal{J}_2 + \mathcal{J}_3. \end{aligned} \quad (23)$$

In the next lemma, we estimate \mathcal{J}_i .

Lemma 4.2. *The terms $\mathcal{J}_i, i = 1, 2, 3$ satisfy*

- (i) $\mathcal{J}_1 = 0$.
- (ii) $\mathcal{J}_2 = -\lambda_1 \int_{(\mathbb{R}^{2d} \times \mathbb{R}_+)^2} k_1(x, y) |v - v_*|^2 f(y, v_*, t; \zeta_*) f(x, v, t; \zeta) d\zeta_* d\zeta dv_* dv dy dx - 2I_0 \int_{\mathbb{R}^{2d} \times \mathbb{R}_+} |v - u_\infty \hat{e}_s|^2 (1 - \varphi(\zeta; \zeta_{cr})) f d\zeta dv dx$.
- (iii) $\mathcal{J}_3 = 0$.

Proof. (i) and (iii). The Divergence theorem implies

$$\mathcal{J}_1 = - \int_{\mathbb{R}^{2d} \times \mathbb{R}_+} \operatorname{div}_x \left(|v - u_\infty \hat{e}_s|^2 v f \right) d\zeta dv dx = 0,$$

$$\mathcal{J}_3 = - \int_{\mathbb{R}^{2d} \times \mathbb{R}_+} \partial_\zeta \left[|v - u_\infty \hat{e}_s|^2 \left(\lambda_2 K_2[f]f + I_0 \varphi(\zeta; \zeta_{cp})f \right) \right] d\zeta dv dx = 0.$$

(ii) In this case, we use the divergence theorem to rewrite \mathcal{J}_2 as

$$\begin{aligned} \mathcal{J}_2 &= 2\lambda_1 \int_{\mathbb{R}^{2d} \times \mathbb{R}_+} (v - u_\infty \hat{e}_s) \cdot K_1[f]f d\zeta dv dx \\ &\quad - 2I_0 \int_{\mathbb{R}^{2d} \times \mathbb{R}_+} |v - u_\infty \hat{e}_s|^2 (1 - \varphi(\zeta; \zeta_{cr}))f d\zeta dv dx. \end{aligned} \quad (24)$$

The first term in (24) can be simplified as follows:

$$\begin{aligned} &2\lambda_1 \int_{\mathbb{R}^{2d} \times \mathbb{R}_+} (v - u_\infty \hat{e}_s) \cdot K_1[f]f d\zeta dv dx \\ &= -2\lambda_1 \int_{(\mathbb{R}^{2d} \times \mathbb{R}_+)^2} k_1(x, y) (v - u_\infty \hat{e}_s) \cdot (v - v_*) \\ &\quad f(y, v_*, t; \zeta_*) f(x, v, t; \zeta) d\zeta_* d\zeta dv_* dv dy dx \end{aligned} \quad (25)$$

The term involving $u_\infty \hat{e}_s$ vanishes due to the symmetry of k_1 with respect to its variable and the anti-symmetry of $(v - v_*)$ with respect to exchanging v and v_* . Hence, the RHS of (25) equals to

$$\begin{aligned} &2\lambda_1 \int_{\mathbb{R}^{2d} \times \mathbb{R}_+} (v - u_\infty \hat{e}_s) \cdot K_1[f]f d\zeta dv dx \\ &\quad - 2\lambda_1 \int_{(\mathbb{R}^{2d} \times \mathbb{R}_+)^2} k_1(x, y) v \cdot (v - v_*) f(y, v_*, t; \zeta_*) f(x, v, t; \zeta) d\zeta_* d\zeta dv_* dv dy dx \\ &= -\lambda_1 \int_{(\mathbb{R}^{2d} \times \mathbb{R}_+)^2} k_1(x, y) |v - v_*|^2 f(y, v_*, t; \zeta_*) f(x, v, t; \zeta) d\zeta_* d\zeta dv_* dv dy dx. \end{aligned} \quad (26)$$

The second equality in (26) holds due to the same symmetry arguments. The desired result can now be obtained by combining (24) and (26). \square

Lemma 4.2 implies that the RHS of (23) is non-positive, i.e.,

$$\frac{d}{dt} \mathcal{F}(f(t)) \leq 0. \quad (27)$$

Clearly, (27) still does not mean that as $t \rightarrow \infty$, $\mathcal{F}(f(t)) \rightarrow 0$, which will imply flocking, i.e., asymptotically identical velocities for all particles. However, at least in the case when the particles are fully excited, we can show that $\mathcal{F}(f(t)) \rightarrow 0$ exponentially fast, as stated by the following lemma:

Lemma 4.3. *Suppose that $I_0 > 0$ and that the particles are fully excited $\forall t > t_*$, i.e.,*

$$\varphi(\zeta; \zeta_{cr}) = 0, \quad t \geq t_*.$$

Then we have

$$\mathcal{F}(f(t)) \leq \mathcal{F}(f(t_*)) e^{-2I_0(t-t_*)}, \quad t \geq t_*.$$

Proof. Since the particles are fully excited, $\varphi = 0$, and hence the RHS of (23) reads

$$\begin{aligned} \frac{d}{dt}\mathcal{F}(f(t)) &= \frac{d}{dt} \int_{\mathbb{R}^{2d} \times \mathbb{R}_+} |v - u_\infty \hat{e}_s|^2 f(x, v, t; \zeta) d\zeta dv dx \\ &= -\lambda_1 \int_{(\mathbb{R}^{2d} \times \mathbb{R}_+)^2} k_1(x, y) |v - v_*|^2 f(y, v_*, t; \zeta_*) f(x, v, t; \zeta) d\zeta_* d\zeta dv_* dv dy dx \\ &\quad - 2I_0 \int_{\mathbb{R}^{2d} \times \mathbb{R}_+} |v - u_\infty \hat{e}_s|^2 f(x, v, t; \zeta) d\zeta dv dx \\ &\leq -2I_0 \mathcal{F}(f(t)). \end{aligned}$$

The result follows by Gronwall's inequality. \square

4.2. Adding collisions with the environment. When there is a velocity jump in the evolution of the one-particle distribution function, its jump process is usually represented by the nonlocal operator which measures the interaction between bacteria and the surface, i.e.,

$$\begin{aligned} \partial_t f + \operatorname{div}_x(vf) + \operatorname{div}_v \left((u_\infty \hat{e}_s - v)(1 - \varphi(\zeta; \zeta_{cr}))f + \lambda_1 K_1[f]f \right) \\ + \partial_\zeta \left(I_0 \varphi(\zeta; \zeta_{cp})f + \lambda_2 K_2[f]f \right) = \left(\frac{\partial f}{\partial t} \right)_c. \end{aligned} \quad (28)$$

The experimental data indicates that bacteria tend to move on areas that were previously traveled on by other bacteria. We denote by $l(x, t)$ the function that represents the surface memory effect (at time t). It increases at x when a bacterium crosses x , and decreases due to a diffusion effect in this memory. Bacteria tend to move towards areas with a higher surface memory. The surface memory effect function, $l(x, t)$, satisfies the nonlinear diffusion equation (with $\eta > 0$, [24]) :

$$\partial_t l = \eta(l, \rho) \Delta l + \lambda(l, \rho) \rho, \quad \text{where } \rho = \int_{\mathbb{R}^d \times \mathbb{R}_+} f d\zeta dv. \quad (29)$$

Before we explicitly write down an equation for $\left(\frac{\partial f}{\partial t} \right)_c$, we briefly explain its motivation. We assumed that the velocity undergoes instantaneous jumps due to the tendency toward higher surface density direction, whereas we assume that the excitation is a continuous process so that it is not involved in the jump process. For the velocity jump process, we employ the finite sampling idea of Hillen-Painter-Schmeiser [19] to model the collision operator. For phototaxis, the surface memory effect due to the background medium is analogous to the role of the chemoattractant in chemotaxis, hence we can employ the similar turning operator as in [19]. We assume that an individual bacterium can measure the surface memory effect along a sphere with radius R around its position x , and bacteria will tend to move in the direction of higher surface density with higher probability. The turning operator is given by

$$\begin{aligned} T[l]f(x, v, t; \zeta) &\equiv \\ &\int_{\mathbb{R}^d} \left[q\left(l\left(x + R \frac{v}{|v|}, t\right)\right) f(x, v', t; \zeta) - q\left(l\left(x + R \frac{v'}{|v'|}, t\right)\right) f(x, v, t; \zeta) \right] dv', \end{aligned} \quad (30)$$

The rate $q(l(x + Rv'/|v'|, t))$ of the jump from the velocity v to v' can be modeled as proportional to the concentration of bound receptor as a function of the medium excitation density l . Hence the term $q(l(x + Rv'/|v'|, t))$ describes the probability

density of choosing a new direction v , given the information $l(x + Rv/|v|, t)$ in that direction.

By combining (28)–(30), we arrive at the following collisional kinetic model:

$$\begin{aligned} \partial_t f + \operatorname{div}_x(vf) + \operatorname{div}_v\left((u_\infty \hat{e}_s - v)(1 - \varphi(\zeta; \zeta_{cr}))f + \lambda_1 K_1[f]f\right) \\ + \partial_\zeta\left(I_0 \varphi(\zeta; \zeta_{cp})f + \lambda_2 K_2[f]f\right) = T[l]f, \\ \partial_t l = \eta \Delta l + \lambda(l, \rho)\rho, \end{aligned} \quad (31)$$

where $\rho = \int_{\mathbb{R}^d \times \mathbb{R}_+} f d\zeta dv$. The non-local operators $K_1[f]$, $K_2[f]$, and $T[l](f)$ are given by (22) and (30).

While it is not shown in the experimental snapshots, Figures 1, 2, & 3, in the experiments we observe irregular and abrupt jumps in the velocities. The collision operators modeling the velocity jump should induce a directional orientation toward the light source. Without accounting for the direction of light in the collision operator, the particles might end up moving in the direction of the local center of mass velocity due to the flocking term, which is not the direction of the light source.

5. The macroscopic limit: The Vlasov-McKean equation. In this section, we derive our third model in the hierarchy of phototaxis models. This model is a macroscopic model that is derived via the formal macroscopic limit of the kinetic model (31). The resulting fluid model will turn to be the Vlasov-McKean equation for the mass density, coupled with a reaction-diffusion equation for the surface memory. Consider the rescaled kinetic model of (31):

$$\begin{aligned} \varepsilon^2 \partial_t f^\varepsilon + \varepsilon \operatorname{div}_x(vf^\varepsilon) + \varepsilon \operatorname{div}_v\left((u_\infty \hat{e}_s - v)(1 - \varphi(\zeta; \zeta_{cr}))f^\varepsilon + \lambda_1 K_1[f^\varepsilon]f^\varepsilon\right) \\ + \varepsilon \partial_\zeta\left(I_0 \varphi(\zeta; \zeta_{cp})f^\varepsilon + \lambda_2 K_2[f^\varepsilon]f^\varepsilon\right) = T^\varepsilon[l^\varepsilon]f^\varepsilon, \\ \partial_t l^\varepsilon = \eta(l^\varepsilon, \rho^\varepsilon)\Delta l^\varepsilon + \lambda(l^\varepsilon, \rho^\varepsilon)\rho^\varepsilon. \end{aligned} \quad (32)$$

We now introduce hydrodynamic quantities (*mass density* and *current density*):

$$\rho^\varepsilon(x, t) := \int_{\mathbb{R}^d \times \mathbb{R}_+} f^\varepsilon d\zeta dv, \quad j^\varepsilon(x, t) := \int_{\mathbb{R}^d \times \mathbb{R}_+} v f^\varepsilon d\zeta dv.$$

We integrate the first equation in (32) over $(v, \zeta) \in \mathbb{R}^d \times \mathbb{R}_+$ to get the continuity equation, to which we add the second equation in (32):

$$\begin{aligned} \varepsilon \partial_t \rho^\varepsilon + \operatorname{div}_x j^\varepsilon &= 0, \\ \partial_t l^\varepsilon &= \eta(l^\varepsilon, \rho^\varepsilon)\Delta l^\varepsilon + \lambda(l^\varepsilon, \rho^\varepsilon)\rho^\varepsilon. \end{aligned} \quad (33)$$

We proceed a formal asymptotic analysis with the following ansatz:

$$\begin{aligned} f^\varepsilon &= f^0 + \varepsilon f^1 + \mathcal{O}(\varepsilon^2), & \rho^\varepsilon &= \rho^0 + \varepsilon \rho^1 + \mathcal{O}(\varepsilon^2), \\ l^\varepsilon &= l^0 + \varepsilon l^1 + \mathcal{O}(\varepsilon^2), & T^\varepsilon[l] &= T^0[l] + \varepsilon T^1[l] + \mathcal{O}(\varepsilon^2). \end{aligned} \quad (34)$$

Our goal is to derive a closed system for the leading order quantities ρ^0, l^0 . We substitute (34) into (33). The leading dynamics for the second equation in (33) can be easily found.

$$\partial_t l^0 = \eta(l^0, \rho^0)\Delta l^0 + \lambda(l^0, \rho^0)\rho^0. \quad (35)$$

On the other hand, it follows from the first equation in (33) that

$$\varepsilon(\partial_t \rho^0 + \varepsilon \partial_t \rho^1 + \mathcal{O}(\varepsilon^2)) + \operatorname{div}_x \left[\int_{\mathbb{R}^d \times \mathbb{R}_+} v f^0 d\zeta dv + \varepsilon \int_{\mathbb{R}^d \times \mathbb{R}_+} v f^1 d\zeta dv + \mathcal{O}(\varepsilon^2) \right] = 0.$$

By comparing the corresponding coefficients in ε , we get

$$\int_{\mathbb{R}^d \times \mathbb{R}_+} v f^0 d\zeta dv = 0 \quad \text{and} \quad \partial_t \rho^0 + \operatorname{div}_x \left[\int_{\mathbb{R}^d \times \mathbb{R}_+} v f^1 d\zeta dv \right] = 0. \quad (36)$$

Hence once we find the relation for f^1 in terms of ρ^0 and l^0 , we are done. For this, we substitute the ansatz (34) into the kinetic equation in (32):

$$\begin{aligned} & \varepsilon^2(\partial_t f^0 + \varepsilon \partial_t f^1 + \mathcal{O}(\varepsilon^2)) + \varepsilon \left[\operatorname{div}_x(v f^0) + \varepsilon \operatorname{div}_x(v f^1) + \mathcal{O}(\varepsilon^2) \right] \\ & \quad + \varepsilon \operatorname{div}_v \left[(u_\infty \hat{e}_s - v)(1 - \varphi(\zeta; \zeta_{cr}))(f^0 + \varepsilon f^1 + \mathcal{O}(\varepsilon^2)) \right. \\ & \quad \left. + \lambda_1 K_1f^0 + \varepsilon f^1 + \mathcal{O}(\varepsilon^2) \right] \end{aligned} \quad (37)$$

$$+ \varepsilon \partial_\zeta \left[I_0 \varphi(\zeta; \zeta_{cp})(f^0 + \varepsilon f^1 + \mathcal{O}(\varepsilon^2)) \right] \quad (38)$$

$$+ \lambda_2 K_2f^0 + \varepsilon f^1 + \mathcal{O}(\varepsilon^2)$$

$$= T^\varepsilon[l^\varepsilon](f^0 + \varepsilon f^1 + \mathcal{O}(\varepsilon^2)).$$

Note that

$$\begin{aligned} & T^\varepsilon[l^\varepsilon](f^0 + \varepsilon f^1 + \mathcal{O}(\varepsilon^2)) \\ & \quad = T^0[l^\varepsilon](f^0 + \varepsilon f^1 + \mathcal{O}(\varepsilon^2)) + \varepsilon T^1[l^\varepsilon](f^0 + \varepsilon f^1 + \mathcal{O}(\varepsilon^2)) + \mathcal{O}(\varepsilon^2) \quad (39) \\ & \quad = T^0[l^0]f^0 + \varepsilon \left(T_l^0[l^0, l^1]f^0 + T^0[l^0]f^1 + T^1[l^0]f^0 \right) + \mathcal{O}(\varepsilon^2), \end{aligned}$$

where $T_l^0[l^0, l^1]$ is a turning operator whose kernel is the Fréchet derivative of T^0 with respect to l , evaluated at l^0 in the direction l^1 . We next compare the $\mathcal{O}(1)$, $\mathcal{O}(\varepsilon)$ terms in (37) using (39) to find

$$\mathcal{O}(1) : T^0[l^0]f^0 = 0, \quad (40)$$

$$\begin{aligned} \mathcal{O}(\varepsilon) : & \operatorname{div}_x(v f^0) + \operatorname{div}_v \left[(u_\infty \hat{e}_s - v)(1 - \varphi(\zeta; \zeta_{cr}))f^0 + \lambda_1 K_1[f^0]f^0 \right] \\ & \quad + \partial_\zeta \left[I_0 \varphi(\zeta; \zeta_{cp})f^0 + \lambda_2 K_2[f^0]f^0 \right] \\ & \quad = T^0[l^0]f^1 + T^1[l^0]f^0. \end{aligned} \quad (41)$$

Here, we used the fact that since the equilibrium distribution is independent of l , the term $T_l^0[l^0, l^1](f^0)$ vanishes. we now take an ansatz for f^0 :

$$f^0(x, v, t; \zeta) = \rho^0(x, t)F(v)\Pi(\zeta). \quad (42)$$

and plug the above ansatz (42) into the equation (41) to find

$$\begin{aligned} T^0[l^0]f^1 & = v \cdot \nabla_x f^0 + \operatorname{div}_v \left[(u_\infty \hat{e}_s - v)(1 - \varphi(\zeta; \zeta_{cr}))f^0 + \lambda_1 K_1[f^0]f^0 \right] \\ & \quad + \partial_\zeta \left[I_0 \varphi(\zeta; \zeta_{cp})f^0 + \lambda_2 K_2[f^0]f^0 \right] - T^1[l^0]f^0 \\ & = \left(vF(v)\Pi(\zeta) \right) \cdot \nabla_x \rho^0 + \operatorname{div}_v \left[(u_\infty \hat{e}_s - v)(1 - \varphi(\zeta; \zeta_{cr}))F(v)\Pi(\zeta) \right] \rho^0 \\ & \quad - \lambda_1 L[\rho^0] \rho^0 \operatorname{div}_v \left[\left(\int_{\mathbb{R}^d} (v - v_*)F(v_*)dv_* \right) F(v)(\Pi(\zeta))^2 \right] \end{aligned}$$

$$\begin{aligned}
& + \partial_\zeta \left[I_0 \varphi(\zeta; \zeta_{cp}) F(v) \Pi(\zeta) \right] \rho^0 \\
& - \lambda_2 \left(F^2(v) \partial_\zeta \left[\int_{\mathbb{R}^+} (\zeta - \zeta_*) G(\zeta_*) d\zeta_* G(\zeta) \right] \right) \rho^0 L[\rho^0] \\
& - \left(T^1[l^0] F(v) \Pi(\zeta) \right) \rho^0.
\end{aligned}$$

Here, the operator L is the convolution operator defined as follows:

$$L[\rho^0](x, t) := \int_{\mathbb{R}^d} r(x, y) \rho^0(y, t) dy.$$

Assuming that $T^0[l^0]$ is invertible, we have

$$\begin{aligned}
f^1 & = \left(T^0[l^0]^{-1} v F(v) \Pi(\zeta) \right) \cdot \nabla_x \rho^0 \\
& + T^0[l^0]^{-1} \operatorname{div}_v \left[(u_\infty \hat{e}_s - v) (1 - \varphi(\zeta; \zeta_{cr})) F(v) \Pi(\zeta) \right] \rho^0 \\
& - \lambda_1 L[\rho^0] \rho^0 T^0[l^0]^{-1} \operatorname{div}_v \left[\left(\int_{\mathbb{R}^d} (v - v_*) F(v_*) dv_* \right) F(v) (\Pi(\zeta))^2 \right] \\
& + T^0[l^0]^{-1} \partial_\zeta \left[I_0 \varphi(\zeta; \zeta_{cp}) F(v) \Pi(\zeta) \right] \rho^0 \\
& - \lambda_2 \left(T^0[l^0]^{-1} F^2(v) \partial_\zeta \left[\int_{\mathbb{R}^+} (\zeta - \zeta_*) G(\zeta_*) d\zeta_* G(\zeta) \right] \right) \rho^0 L[\rho^0] \\
& - \left(T^0[l^0]^{-1} T^1[l^0] F(v) \Pi(\zeta) \right) \rho^0.
\end{aligned} \tag{43}$$

We now substitute f^1 into the equation (36) to see

$$\partial_t \rho^0 = \operatorname{div}_x \left(D(l^0) \nabla_x \rho_0 + C_1(l^0) \rho^0 L[\rho^0] + C_2(l^0) \rho^0 \right),$$

where

$$\begin{aligned}
D(l^0) & := - \int_{\mathbb{R}^d \times \mathbb{R}^+} v \otimes (T^0(l^0)^{-1} v F(v) \Pi(\zeta)) d\zeta dv, \\
C_1(l^0) & := \int_{\mathbb{R}^d \times \mathbb{R}^+} v \left\{ \lambda_1 T^0[l^0]^{-1} \operatorname{div}_v \left[\left(\int_{\mathbb{R}^d} (v - v_*) F(v_*) dv_* \right) F(v) (\Pi(\zeta))^2 \right] \right. \\
& \quad \left. + \lambda_2 \left(T^0[l^0]^{-1} F^2(v) \partial_\zeta \left[\int_{\mathbb{R}^+} (\zeta - \zeta_*) G(\zeta_*) d\zeta_* G(\zeta) \right] \right) \right\} d\zeta dv, \\
C_2(l^0) & := - \int_{\mathbb{R}^d \times \mathbb{R}^+} v \left\{ T^0[l^0]^{-1} \operatorname{div}_v \left[(u_\infty \hat{e}_s - v) (1 - \varphi(\zeta; \zeta_{cr})) F(v) \Pi(\zeta) \right] \right. \\
& \quad \left. + T^0[l^0]^{-1} \partial_\zeta \left[I_0 \varphi(\zeta; \zeta_{cp}) F(v) \Pi(\zeta) \right] - \left(T^0[l^0]^{-1} T^1[l^0] F(v) \Pi(\zeta) \right) \right\} d\zeta dv.
\end{aligned}$$

This completes the derivation of the fluid model. To summarize, the third model in the hierarchy of phototaxis models is of the form of the Vlasov-McKean equation coupled with a reaction-diffusion equation:

$$\begin{aligned}
\partial_t \rho & = \operatorname{div}_x \left(D(l) \nabla_x \rho + C_1(l) \rho L[\rho] + C_2(l) \rho \right), \quad (x, t) \in \mathbb{R}^d \times \mathbb{R}_+, \\
\partial_t l & = \eta(l, \rho) \Delta l + \lambda(l, \rho) \rho.
\end{aligned} \tag{44}$$

Remark 9. The derivation of the fluid model (44) was done using formal asymptotic expansion arguments. The rigorous justification of this limit is beyond the scope of this paper and is left for future work.

6. Conclusion. In this work we derived a hierarchy of new mathematical models for phototaxis. The recent experiments of Burriesci and Bhaya [10] indicated that the motion of the phototactic bacteria depends on a variety of parameters in addition to the light source: the individual characteristics of each bacterium, interaction between neighboring bacteria, and interactions between the bacteria and the environment in which they operate.

The first model in the hierarchy is a collisionless particle system that can be viewed as an extension of the Cucker-Smale flocking model that incorporates a non-linear internal dependence of the dynamics on one of the variables (excitation), as well as external forces (for the velocity and for the excitation).

The second model is a kinetic model that was derived from the particle system. The interaction between bacteria and the environment was incorporated into the kinetic model via the turning operator that accounts for such collisions. This interaction, which is reflected by velocity jumps, is due to the observation that bacteria prefer to move in areas that were previously traveled on by other bacteria, a phenomenon which we refer to as a “surface memory effect”.

The third model is a fluid model that was formally derived as the macroscopic limit of the kinetic model. The resulting model turned out to be the Vlasov-McKean equation coupled with a reaction-diffusion equation (for the surface memory effect).

The theoretical results established the expected flocking behavior for the particle system and for the kinetic model, at least for the case where all particles are fully excited so that excitation does not affect the dynamics of the position and velocity. We then proved that the canonical asymptotic behavior of the particle system is such that it always reaches a state where all particles are fully excited.

There are several issues that are left for future work: from a modeling perspective it is natural to add random fluctuations to the model. Also missing from the present models are sensitivity to light, and allowing for the population of bacteria to change over time. It will probably be a good idea to also add directionality considerations in the parameters that control the motion (e.g., to limit the role of information that propagates from the direction opposite to the direction of motion and/or the direction of light).

The numerical simulations that were conducted in this paper were done only for the (collisionless) particle system. It will be interesting to simulate the solutions of the kinetic model and of the fluid model. This is a non-trivial task that is left for a future study.

From a theoretical point of view, there are many open problems. The fundamental question of justifying the molecular question assumption is as hard here as it is for the Boltzmann equation. The derivation of the fluid model from the kinetic model was done following formal arguments and should also be rigorously justified. These questions are left for future considerations.

It also remains to connect some of the observations with the model. While Observation #1 regarding the delayed motion and Observation #4 regarding the surface memory effect are directly encoded into the model, Observation #2 (fingering) is expected to be a macroscopic observable as we have shown for other models in [7, 24, 25]. It is left for future work to explore whether any of the models that were developed in this work can actually generate such a macroscopic dynamics. Observations #3 and #5 regarding the density-dependent motion and the sensing of other bacteria, can be controlled by adjusting the communication rates. A detailed study is left to a future work.

Acknowledgments. This research was carried out when S.-Y. Ha was visiting the Department of Mathematics at the University of Maryland in College Park, and it is a great pleasure to thank the faculty of the Applied Mathematics group for their hospitality.

REFERENCES

- [1] J. P. Armitage, *Bacterial tactic responses*, Adv. Microb. Physiol., **41** (1999), 229–289.
- [2] N. Bellomo and M. Pulvirenti, “Modeling in Applied Sciences: A Kinetic Theory Approach,” Birkhäuser, Boston, 2000.
- [3] A. Bellouquid and M. Delitala, “Mathematical Modeling of Complex Biological Systems: A Kinetic Theory Approach,” Birkhäuser, Boston, 2006.
- [4] D. Benedetto, E. Caglioti and M. Pulvirenti *A kinetic equation for granular media*, RAIRO Modél. Math. Anal. Numér. , **5** (1997), 615–641.
- [5] D. Bhaya, *Light matters: Phototaxis and signal transduction in unicellular cyanobacteria*, Mol. Microbiol., **53** (2004), 745–754.
- [6] D. Bhaya, N. R. Bianco, D. Bryant and A. R. Grossman, *Type IV pilus biogenesis and motility in the cyanobacterium Synechocystis sp. PCC6803*, Mol. Microbiol., **37** (2000), 941–951.
- [7] D. Bhaya, D. Levy and T. Requeijo, *Group dynamics of phototaxis: Interacting stochastic many-particle systems and their continuum limits*, in “Hyperbolic Problems: Theory, Numerics, Applications” (eds. S. Benzoni-Gavage and D. Serre), Springer-Verlag, Berlin, 145–159, 2008.
- [8] D. Bhaya, A. Takahashi, P. Shahi and A. R. Grossman, *Light regulation of type IV pilus-dependent motility by chemosensor-like elements in synechocystis PCC 6803*, Proc. Natl. Acad. Sci. U.S.A., **98** (2001), 7540–7545.
- [9] D. Bhaya, A. Takahashi, P. Shahi and A. R. Grossman, *Novel motility mutants of Synechocystis strain PCC 6803 generated by in vitro transposon mutagenesis*, J. Bacteriol., **183** (2001), 6140–6143.
- [10] M. Burriesci and D. Bhaya, *Tracking phototactic responses and modeling motility of Synechocystis sp. Strain PCC6803*, J. Photochem. Photobio., **91** (2008), 77–86.
- [11] L. L. Burrows, *Weapons of mass retraction*, Mol. Microbiol., **57** (2005), 878–888.
- [12] F. Chalub, P. Markowich and B. Perthame, *Kinetic models for chemotaxis and their drift-diffusion limits*, Monatsh. Math., **142** (2004), 123–141.
- [13] S. Chapman and T. G. Cowling, “The Mathematical Theory of Non-Uniform Gases,” Cambridge University Press, Cambridge, UK, 1990.
- [14] S. Childress, M. Levandowsky and E. A. Spiegel, *Pattern formation in a suspension of swimming microorganisms: Equations and stability theory*, J. Fluid Mech., **69** (1975), 591–613.
- [15] F. Cucker and S. Smale, *On the mathematics of emergence*, Japan. J. Math., **2** (2007), 197–227.
- [16] F. Cucker and S. Smale, *Emergent behavior in flocks*, IEEE Trans. Automat. Control, **52** (2007), 852–862.
- [17] S.-Y. Ha and J. G. Liu, *Short proof of Cucker-Smale’s flocking and the mean-field limit*, Comm. Math. Sci., to appear.
- [18] S.-Y. Ha and E. Tadmor, *From particle to kinetic and hydrodynamics description of flocking*, Kinet. Relat. Modelins, **1** (2008), 415–435.
- [19] T. Hillen, K. Painter and C. Schmeiser, *Global existence for chemotaxis with finite sampling radius*, Disc. Cont. Dyn. Sys. B, **7** (2007), 125–144.
- [20] D. Horstmann, *From 1970 until present: The Keller-Segel model in chemotaxis and its consequences I*, Jahresberichte der DMV , **105** (2003), 103–165.
- [21] E. F. Keller and L. A. Segel, *A model for chemotaxis*, J. Theor. Biology, **30** (1971), 225–234.
- [22] E. F. Keller and L. A. Segel, *Travelling bands of chemotactic bacteria: A theoretical analysis*, J. Theor. Biology, **30** (1971), 235–248.
- [23] E. H. Kennard, “Kinetic Theory of Gases,” McGraw-Hill, New York and London, 1938.
- [24] D. Levy and T. Requeijo, *Modeling group dynamics of phototaxis: From Particle systems to PDEs*, Disc. Cont. Dyn. Sys. B , **9** (2008), 108–128.
- [25] D. Levy and T. Requeijo, *Stochastic models for phototaxis*, Bull. Math. Bio., **70** (2008), 1684–1706.
- [26] R. L. Liboff, “Introduction to the Theory of Kinetic Equations,” John Wiley, New York, 1969.

- [27] A. Maree, A. Panfilov and P. Hogeweg, *Phototaxis during the slug stage of Dictyostelium discoideum: A model study*, Proc. Royal Soc. Lond. B, **266** (1999), 1351–1360.
- [28] A. Maree, A. Panfilov and P. Hogeweg, *Phototaxis during the slug stage of Dictyostelium discoideum: A model study*, Proc. R. Soc. Lond. B, **266** (1999), 1351–1360.
- [29] S. Masuda and T. A. Ono, *Adenylyl cyclase activity of Cya1 from the cyanobacterium Synechocystis sp. strain PCC 6803 is inhibited by bicarbonate*, J. Bacteriol., **187** (2005), 5032–5035.
- [30] S. Masuda and T. A. Ono, *Biochemical characterization of the major adenylyl cyclase, Cya1, in the cyanobacterium Synechocystis sp. PCC 6803*, FEBS Lett., **577** (2004), 255–258.
- [31] J. S. Mattick, *Type IV pili and twitching motility*, Annu. Rev. Microbiol., **56** (2002), 289–314.
- [32] M. Ohmori and S. Okamoto, *Photoresponsive cAMP signal transduction in cyanobacteria*, Photochem. Photobiol. Sci., **3** (2004), 503–511.
- [33] C. S. Patlak, *Random walk with persistence and external bias*, Bull. Math. Biophys., **15** (1953), 311–338.
- [34] B. Perthame, “Transport Equations in Biology,” Frontiers in Mathematics, Birkhäuser Verlag, Basel, 2007.
- [35] G. Russo and P. Smereka, *Kinetic theory for bubbly flow. II. Fluid dynamic limit*, SIAM J. Appl. Math., **56** (1996), 358–371.
- [36] G. Russo and P. Smereka, *Kinetic theory for bubbly flow. I. Collisionless case*, SIAM J. Appl. Math., **56** (1996), 327–357.
- [37] J. Shen, *Cucker-Smale flocking under hierarchical leadership*, SIAM J. Appl. Math., **68** (2007), 694–719.
- [38] J. M. Skerker and H. C. Berg, *Direct observation of extension and retraction of type IV pili*, Proc. Natl. Acad. Sci. USA, **98** (2001), 6901–6904.
- [39] K. Terauchi and M. Ohmori, *An adenylate cyclase, Cya1, regulates cell motility in the cyanobacterium Synechocystis sp. PCC 6803*, Plant Cell Physiol., **40** (1999), 248–251.
- [40] S. Yoshihara and M. Ikeuchi, *Phototactic motility in the unicellular cyanobacterium Synechocystis sp. PCC 6803*, Photochem. Photobiol. Sci., **3** (2004), 512–518.
- [41] H. Yoshimura, S. Yanagisawa, M. Kanehisa and M. Ohmori, *Screening for the target gene of cyanobacterial cAMP receptor protein SYCRP1*, Mol. Microbiol., **43** (2002), 843–853.
- [42] H. Yoshimura, S. Yoshihara, S. Okamoto, M. Ikeuchi and M. Ohmori, *A cAMP receptor protein, SYCRP1, is responsible for the cell motility of Synechocystis sp. PCC 6803*, Plant Cell Physiol., **43** (2002), 460–463.

Received March 2008; revised February 2009.

E-mail address: syha@snu.ac.kr

E-mail address: dlevy@math.umd.edu